2014

Potential Optimal Gait Performance of Mauch S-N-S Prosthetic Knee Configurations as Predicted by Dynamic Modeling

Chih-hao Chien
Cleveland State University

POTENTIAL OPTIMAL GAIT PERFORMANCE OF MAUCH S-N-S PROSTHETIC KNEE CONFIGURATIONS AS PREDICTED BY DYNAMIC MODELING

CHIH-HAO CHIEN

Bachelor of Mechanical Engineering
TamKang University, Taiwan
June 2002

Master of Science in Mechanical Engineering
Cleveland State University
August 2007

submitted in partial fulfillment of requirement for the degree
DOCTOR OF ENGINEERING
at the
CLEVELAND STATE UNIVERSITY
August 2014

We hereby approve this thesis of

Chih-Hao Chien

Candidate for the Doctor of Engineering in Applied Biomedical Engineering degree for the

Department of Chemical and Biomedical Engineering

and the CLEVELAND STATE UNIVERSITY

College of Graduate Studies

Thesis Chairperson, William A. Smith, Ph.D.

Chemical and Biomedical Engineering May 2, 2014
Department & Date

Thesis Committee Member, Nolan B. Holland, Ph.D.

Chemical and Biomedical Engineering May 2, 2014
Department & Date

Thesis Committee Member Brian L. Davis, Ph.D.

The University of Akron May 2, 2014
Department & Date

Thesis Committee Member, Howard Paul, Ph.D.

Computer & Information Sciences May 2, 2014
Department & Date

Thesis Committee Member Ton van den Bogert, Ph.D.

Mechanical Engineering May 2, 2014
Department & Date

Thesis Committee Member Aimin Zhou, Ph.D.

Chemistry May 2, 2014
Department & Date

Thesis Committee Member Dan J. Simon, Ph.D.

Electrical & Computer Engineering May 2, 2014
Department & Date

Student's Date of Defense: Friday, May 2, 2014

POTENTIAL OPTIMAL GAIT PERFORMANCE OF MAUCH S-N-S PROSTHETIC KNEE CONFIGURATIONS AS PREDICTED BY DYNAMIC MODELING

CHIH-HAO CHIEN

ABSTRACT

Patients with prosthetic legs routinely suffer from abnormal gait patterns which can cause health issues and eventually lower the quality of their lives. Despite the half-century advance in the technology of prosthetic knees, from the purely mechanical to microprocessor controlled systems, patient testing suggests that very little progress has been made in the quality of the kinetics and kinematics of amputee gait. Moreover, the cost of microprocessor controlled prosthetic knees may be 10 times more than the purely mechanical knees. While prosthetic knees have become more complex and expensive, it is not proven that the prosthetic knee is a central factor limiting amputee patient gait.

The goal of this project is to determine the degree to which the Mauch S-N-S prosthetic knee limits the ability of a subject to achieve a close to normal gait pattern. In this research, we developed dynamic models of the Mauch S-N-S prosthetic knee based on gait-like motion tests of a Mauch knee cylinder and used the dynamic models in computational simulations to determine the best achievable gait, on the basis of obtaining near-to-normal gait kinematics and kinetics. Idealized assumptions were made for patient performance capability and characteristics of the other prosthetic leg components, to obtain the desired focus on knee capabilities and limitations. The results indicate that even with this relatively old technology prosthetic knee, subjects have the potential to walk much more normally than the patient-test data indicates. An extension of the study showed the significant interaction of the prosthetic knee and ankle with respect to

achieving optimal gait. The methodology of this study can be applied to evaluation other knees, prosthetic components and prosthetic systems combining these components.

TABLE OF CONTENTS

LIST OF FIGURES

LIST OF TABLES

CHAPTER I

INTRODUCTION

1.1 Problem Statement

Loss of a leg, especially above the knee, is a disabling condition that impacts patient mobility and ability to carry out many of the basic activities of life. As far back as the ancient Egyptian dynasties attempts were made to fabricate prosthetic legs similar to natural legs (Norton, K. M., 2007). All too often, warfare has stimulated the development of prosthetic legs and their components (Vanderwerker, E. E., 1976). The development of the "Mauch" knee now supported by Ossur (Reykjavik, Iceland) began after the Second World War (Mauch, H. A. 1958 & 1968). In the intervening years, prosthetic knees of increasing sophistication and modernization have been developed ((Martinez-Villalpando, 2009, Martin, 2003, & Orendurff et al., 2006). However, amputee patients' gait has not significantly improved with the availability of higher technology, more expensive prosthetic knees. This has led us to question if it is the capabilities of the knee which limit patient gait, or if other factors should receive deeper research and development effort. Answering this question requires definition of the capabilities of prosthetic knees, independent of the other components of a prosthetic leg.

1.2 Method of Solution

To meet this need, we have developed a systematic approach for prosthetic knee performance determination, and used it to study the potential performance of the Mauch S-N-S prosthetic knee. This purely hydraulic prosthetic knee design is one of the most widely used devices today, despite its older technology.

The first step of this approach is to use knowledge of gait conditions and the basic principles of the device's function embodied in the patent and other literature to develop a laboratory test exercising the knee over a relevant range of motion to develop a database of experimental input and output parameter sets for the tested hardware. The second step is to employ coefficient estimation techniques to develop mathematical models of the knee based on its experimental dynamic performance.

Third, the prosthetic knee mathematical model is incorporated into a musculoskeletal model to simulate the potential walking pattern of the amputee, idealizing all other factors of the prosthesis. The prosthetic ankle/foot is modeled as a torsional spring (Palmer, M., 2002). For the purposes of this study, the transmission of the forces and moments by the socket is considered to be perfectly transmitted without any loses between the residual hip and the prosthetic leg. In order to simulate a transfemoral amputee, we "amputate" the muscles of the knee and ankle joint in the musculoskeletal model. Because of the limitations of the musculoskeletal model chosen, the function of the residual hip and trunk muscles and the weight of the prosthetic leg are assumed to match the subject's sound side to determine the closest to normal gait kinematics, given the limitations of the knee.

As the fourth and final step of the knee performance evaluation, robotic testing evaluates the realism of the computational simulations under conditions similar to the simulation assumptions.

As an extension of the study, additional simulations varying prosthetic knee operational settings and ankle stiffness assumptions were performed to evaluate how the combination of prosthetic knee settings and ankle stiffness interact to achieve the most normal gait pattern possible with the analysis assumptions made.

1.3 Basic Results

With the integration of the mathematical models of the Mauch knee and the amputated musculoskeletal model, the potential gait pattern of a patient has been determined, for the assumptions of an ideal socket, ankle, rehabilitation training and so forth. The simulation results have shown the potential gait patterns of the subject with the Mauch S-N-S knee are much closer to human normal, with reasonable kinetic and kinematic performance, than are currently achieved by most human amputee subjects.

Robotic testing shows that the simulations achieve reasonable results as compared to controlled test data, despite the limitations of the computational models.

The knee/ankle study reveals that properly matching the prosthetic knee and ankle can improve the potential gait kinetics and kinematics of a transfemoral amputee. The knee by itself is not a major limiting factor in amputee gait performance.

This methodology can be applied to other knees to determine their performance capabilities and potentially to optimize their design and complexity/reliability/cost characteristics while assuring that good gait is a realistic possibility. Other prosthetic components and complete systems can also be modeled and simulated by adapting the

procedures. Simulations can supplement human subject testing and may have a future role guiding the configuration and set up of prosthetic legs for patients and support their rehabilitation.

CHAPTER II

BACKGROUND AND SIGNIFICANCE OF THE RESEARCH PROJECT

This chapter gives a general review of a number of related fields that provide context and background to the proposed research. These include a general background of prosthetic leg development, the causes, consequences, incidence and prevalence of amputation, and an introduction to the prosthetic leg as a whole and to the knee in particular. Modern knees are described with particular attention to the construction and function of the Mauch knee used as a study object here, and the published patient data which motivated this project is outlined.

2.1 Historical Background

The first recorded prosthetic leg was built before 1800 B.C.; it was used by Queen Vishpla, who had lost her leg in battle and wanted to return to active leadership of her troops. (Vanderwerker, 1976). References to such devices become slightly more common in medieval times, when simple “peg legs” were fabricated to help injured warriors ride their horses into combat (Norton, 2007). These were generally

heavy and not particularly functional; only the richest of amputees could afford to have prosthetic legs fabricated that would have some value in daily life. In the 16th century, the work of Ambroise Pare was notable for introducing an iron leg with an articulated knee joint (Seith, 1972), and he also developed more modern concepts of amputation surgery which made the fitting of prosthetic limbs more practical. Further advances were slow until the 19th century when the combination of the Industrial Age, modern warfare, and American programs to provide veteran's benefits to injured Civil War veterans stimulated entrepreneurs to offer lighter weight, better appearing, and better functioning devices (Adalarasu et al, 2011).

The First World War did not stimulate equivalent progress in prosthetic devices, perhaps because fewer American casualties were involved and Europe experienced first the issues of post-war reconstruction and then the Great Depression. After the Second World War, veterans who saw incredible technical progress in weapons development called for similar effort in medical appliances, which resulted in a program of development organized by the National Academy of Sciences utilizing many defense contractors and a number of war booty German scientists (Wilson, 1963). Significant new technology in all aspects of prosthetic limbs came of this effort, notably for this research program the Mauch S-N-S hydraulic knee (Mauch, 1958 & 1968) which remains a mainstay of the field today. In the early 1990's Blatchford introduced the microprocessor controlled pneumatic-hydraulic Intelligent Knee. In the late 90's this morphed into the Adaptive Knee, while Otto Bock brought out the purely hydraulic, microprocessor controlled "C-leg" (Otto Bock HealthCare GmbH, Duderstadt, Germany). Ossur (Reykjavik, Iceland) introduced the "RheoKnee", which uses a magnetic fluid clutch to

provide damping instead of a hydraulic or pneumatic cylinder, and also the "Power Knee" a ball screw driven knee system which could actively power gait, as well as damped leg motion.

2.2 Prevalence, Incidence and Consequences of Amputation/Prosthetic Leg Use

It has been reported that 266,465 people had a transfemoral amputation from 1988 to 1996 (Dillingham et al. 2002). More than 95% of the amputations were caused by peripheral vascular disease and less than 4% were caused by trauma. Diabetes, a major cause of peripheral vascular disease, has been described as a new epidemic, with the number of diagnosed adults tripling between 1980 and 2005; one third of Americans may be diabetic by 2050 (US Center of Disease Control and Prevention, 2011), and 60% of non-traumatic lower extremity amputations were caused by diabetes (Centers for Disease Control and Prevention, 2011). The Center of Disease Control and Prevention statistics also suggest that about 10,000 diabetes-related transfemoral amputations take place each year, suggesting a 16,000-17,000 annual total of new transfemoral amputations. Without effective arrest of the growth of diabetes and treatment of its complications, this number has an unfortunately high growth potential. Transfemoral amputation not only reduces the quality of patients' life, but also accelerates additional deterioration of their concurrent health condition (Kulkarni, 2008). One class of issues derives from the difficulty of walking with a prosthetic leg; it has been estimated that the oxygen consumption of ambulation with a prosthetic leg is 60-100% higher than with a normal leg (Smith., 2004). Patients also have reduced neuromuscular feedback and control (Wentink et al., 2009), reducing the security of balance and increasing the probability of falls. These limitations

encourage inactivity which exacerbates diabetes, heart disease and other metabolically related conditions.

Another set of issues is that patients using prostheses to compensate for lower extremity amputation are at high risk of pathological problems such as osteoarthritis (Burke et al., 1978) and lower back pain (Ehde et al., 2001). They infer that these problems may be caused by asymmetric gait patterns forced by prosthesis limitations or patient rehabilitation issues, as have been extensively discussed in the literature. Researchers (Hof et al., 2007) have found that patients walking with a prosthetic leg have a shorter stance time on the prosthetic side than on the sound side. Additionally the center of pressure (CoP) at foot contact for the prosthetic side is further away from the center of mass (CoM) than on the sound side. Farahmand et al. (2006) have reported that an amputee's sound side hip joint experiences larger extension hip moment and flexion knee moment than a healthy subject while the hip joint of the amputated side experienced lower than normal extension hip moment. It also has been reported that the sound limb muscle activity and co-activity of level walking by amputee patients are greater than healthy subjects (Bae et al., 2007). Specifically, the adductor muscles (of the amputated limb in the stance phase and abductor muscles in swing phase were weakened and generated significantly less muscle force during level walking.

2.3 Description of A Modern Prosthetic Leg

A prosthetic leg for a transfemoral amputee consists of a number of important subsystems (figure 1). The socket (Bechtol, 1951) serves to transmit force and motion between the patient and the prosthesis, and to retain the prosthesis in place on the patient. Sockets have some significant issues with respect to preventing relative motion between

the socket liner and patient skin, transferring forces painlessly between prosthesis and patient, and dissipating heat and moisture at the skin/socket interface (Mak et al., 2001). The biological knee (Schaffer et al., 2008) is a hinge joint with a crucial role in ambulation; most of the time the natural knee absorbs (damps) energy (Winter, 1983), but at key points in the stride it helps extend the knee, lifting the body in late stance and thrusting the knee forward during the stance flexion phase. The vast majority of current clinically available hardware only duplicates the damping function of the natural knee, leaving it to the patient to force knee extension with residual hip muscles. A pylon, or shank, connects the knee to the prosthetic foot. Different prosthetic foot designs have a wide range of sophistication, with a large variation stiffness behavior and in some cases design features to simulate to a greater or lesser extent the energy storage and release ankle functions (Edelstein, 1988). The component of particular interest to this study is the prosthetic knee

Figure 1: Prosthetic leg. From top to bottom: socket, knee, shank, and foot/ankle

2.4 Overview of Current Prosthetic Knees

Knee designs come in varying levels of complexity. For centuries, the carved wood peg leg was a standard (Norton,2007). Hinged knees were known in the Renaissance era, but did not become common until the mid-19th century. Sometimes a braking feature would be included. The basic modern knees have "polycentric" hinging, using a linkage mechanism between upper and lower knee components in contrast to early knees which had a simple rotational axis equivalent to a door hinge. The polycentric configuration provides advantages with respect to ground clearance during ambulation. The polycentric knees (Hobson & Torfason, 1975) usually have friction based braking or damping mechanisms, although hydraulic or pneumatic designs are known. Most "training" knees are simple polycentric designs, and many patients never progress beyond them.

While some polycentric knees are promoted for high activity levels (Yokogushi et al., 2004; Pfeifer et al., 2012), most high performance knees have a single axis of rotation with added mechanisms to modulate performance. Hydraulic cylinders are commonly used to establish resistance to rotation, although other approaches are known, including hybrid hydraulic/pneumatic systems (Pritham, 1983), magnetorheological (MR) fluid systems (Gudmundsson et al., 2011), and motorized systems (Power Knee, Ossur, Reykjavik, Iceland). Early hydraulically controlled knees used various configurations of linkages and/or orifices to cause the main hydraulic valves to open and close at appropriate points in the gait cycle, while new products use microprocessors to read sensor signals and control the operation of solenoid valves to provide more sophisticated damping functions during ambulation.

2.5 Operation of the Mauch Knee

To develop and demonstrate the methodology of this knee investigation, we used a state-of-art mechanically controlled hydraulic prosthetic knee, Mauch Swing'N'Stance (S-N-S) (figure 1). This hardware was developed and for a long time commercialized by Mauch Laboratories in Dayton, Ohio; it is now sold by Ossur (Reykjavik, Iceland). Hans Mauch has described the construction and function of the design (Mauch, 1968). The hardware functions to provide high resistance to knee flexion during stance phase and lower resistance during other gait phases. Externally, the user has access to two adjusting dials which respectively modify the level of damping during knee extension and during flexion. For data recording during this research, we defined extension dial adjustments as "E" and flexion adjustments as "F". The minimum setting in each case was 0, maximum was 180, and 90 was the midpoint. Internally, a valve and balance wheel-based mechanism establish the knee state as swing or stance, and flexion or extension. This arrangement is sensitive to flow direction, viscosity, inertia, and gravity. Based on earlier configurations, it is sometimes known as the "pendulum valve" but with the design implemented in current clinical hardware any probable gait angulation of the knee has a minor effect on the gravitational force on the balance wheel. During stance flexion, the valve is free to close the main orifices and the hydraulic fluid can only flow through small cut-outs around the piston which establish the high resistance to knee flexion during stance phase. When/if the knee is driven to a hyperextension state, the hydraulic piston impacts on a pawl which then lifts, allowing the balance wheel to rotate. The new balance wheel position blocks valve stem motion and prevents valve closure. This hyperextension mode requires a meaningful period of time, 1/10 second in Mauch's

estimate, for the balance wheel to rotate far enough to stop the valve from closing. This situation is most probable at end stance; hyperextension at end swing is possible but is not likely to persist long enough for the mechanism to act. Inertia and viscous drag establish the delay time. High extension flows hold the valve open and valve stem pressure prevents the balance wheel from rotating back into the pawl- locked position after the hyperextension state is exited until extension flow through the valve stops and the valve poppet drops away from the balance wheel. Without hyperextension, the pawl can lock the balance wheel in place.

This hyperextension state requirement is an abnormal gait condition inherently necessary to make the Mauch knee function as designed. Therefore absolutely normal gait patterns cannot be used in the laboratory to characterize the dynamic performance of the design, and an amputee cannot have absolutely normal gait and also obtain the benefits of resistance variation as built into this knee.

CHAPTER III

QUALITATIVE AND QUANTITATIVE ASPECTS OF HUMAN GAIT

To quantify the quality of the gait pattern of a transfemoral amputee wearing a prosthetic leg, the average gait pattern of healthy subjects has to be defined. This chapter is a brief review of the state-of-the-art with respect to defining normal gait.

3.1 The "Gait Cycle" Qualitatively Described

Human locomotion, the gait, is a cyclic process which begins with a foot in contact with the ground surface and ending as the same foot returns to contact. It also is complex process involving the interaction of many muscle groups and sensory systems.

Seven events (Whittle, 2007) have been defined during the gait cycle (figure 2); (1) Initial contact, (2) Opposite toe off, (3) Center of gravity over base of support, (4) Opposite initial contact, (5) Toe off, (6) Maximal knee flexion, and (7) Tibia vertical. The first four events occur during the stance phase, which occupies 60% of a gait cycle and is further divided into (1) Loading response, (2) Mid-stance, (3) Terminal stance, and (4) Pre-swing. The last three events of a gait cycle occur in

the swing phase, which consumes 40% of a gait cycle and is divided into (1) Initial swing, (2) Mid-swing, and (3) Terminal swing.

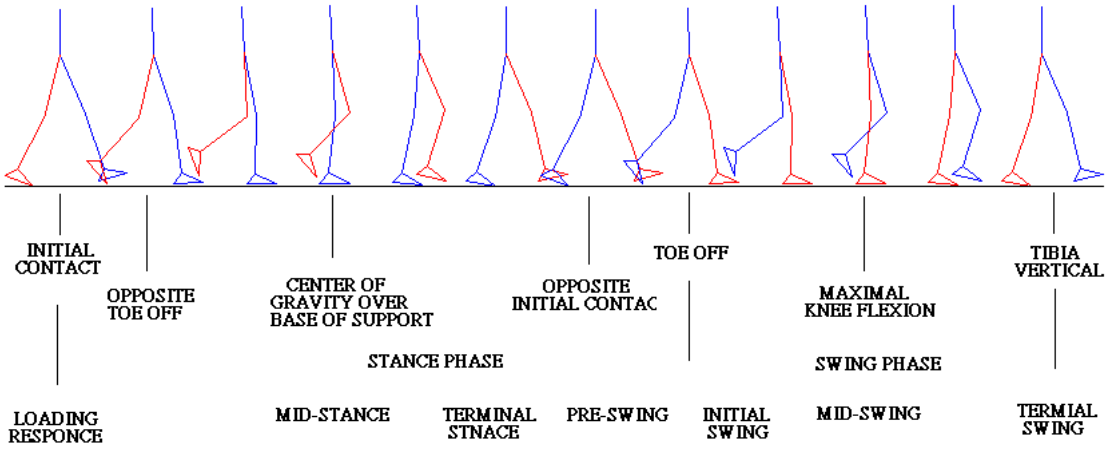

Figure 2: Gait cycle

The actions of multiple body segments must be integrated to complete the motion of ambulation. Six factors of the body segment movements have been defined as the major determinants of gait (Saunders et al., 1953) working together to minimize energy consumption, maintaining a sinusoidal pathway of low amplitude for the center of gravity of the body. (1) Pelvic rotation (lateral rotation of the pelvis), (2) Pelvic tilt (frontal plane rotation of the pelvis), (3) Knee flexion in the stance phase (knee sagittal rotation), (4) Foot mechanism (foot motion and dynamics during stance phase), (5) Knee mechanisms (knee motion and dynamics during stance phase), and (6) Lateral displacement of the pelvis (produced by relative adduction at the hip). However, in the case of a transfemoral amputee, many of the muscle groups co-operating to produce gait motion have been removed and replaced by a prosthesis. Hence amputees have lost much of the normal controllability of their gait. The behavior of the prosthetic leg is dependent on its own mechanical design and control principles.

3.2 Gait Quantitatively Described

The gait is normally quantified by studying its kinematics and kinetics. Kinematics covers displacements, velocities and accelerations of motion, while kinetics studies the forces and energy flows involved in that motion. Movement of the legs is induced by multiple forces and moments acting on the segments of the lower extremity, which include the muscle forces, gravitational effects, and inertial effects. Forces and moments are important descriptors of a subject's gait pattern; they lead to the accelerations, velocities and displacements which describe the kinematics of gait. Gait is a three dimensional phenomenon, but, in general, normal gait is dominated by two dimensional components. Therefore it is reasonable to approximate normal gait with a simpler 2-dimensional model of a leg to illustrate the dynamics of the lower extremity (Winter, 2005). The leg is separated into three segments; the foot-ankle segment, the ankle-shank-knee segment, and the knee-thigh-hip segment. The dynamic equations for estimating the kinetics and kinematics are as below;

(1) The dynamics of the foot-ankle segment

From figure 3, based on force equilibrium, we have

$$\sum F_x = ma_{fx} \qquad ma_{fx} = R_{ax} - R_x \tag{3.1}$$

$$\sum F_y = ma_{fy} \qquad ma_{fy} = R_{ay} + R_y - W_f \tag{3.2}$$

and using moment equilibrium at the ankle joint, we have

$$\sum M_{com} = Ia_{com}\alpha_f$$

$$NJM_a + R_y \times d1 + R_x \times d2 - R_{ay} \times d3 - R_{ax} \times d4 + W \times d5 = Ia_{com}\alpha \tag{3.3}$$

where d1, d2, d3, d4, and d5 are moment arms applicable to each force element respectively.

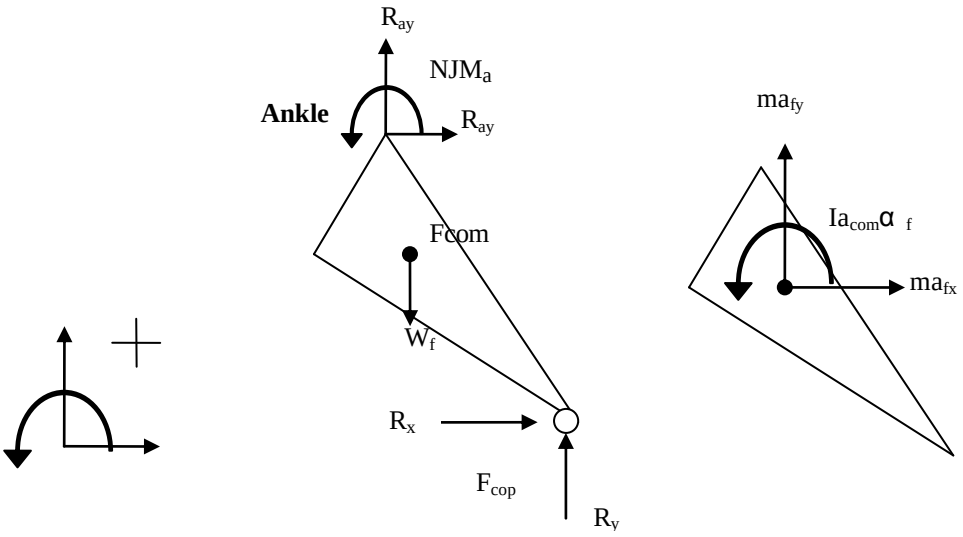

R_{ay}: Horizontal ankle reaction force
R_{ax}: Vertical ankle reaction force
R_x: Horizontal ground reaction force
R_y: Vertical ground reaction force
Fcom: Center of mass of foot
NJM_a: Net ioint moment of ankle
F_{cop}: Center of pressure of foot
ma_{fx}: Horizontal mass acceleration of foot
ma_{fy}: Vertical mass acceleration of foot
Ia_{com}: Mass inertia of ankle
α_f: Angular acceleration of foot
W_f: Weight of foot due to gravity

Figure 3: Free-body diagram of the ankle joint and foot

(2) The dynamics of the ankle-shank

From figure 4, based on force equilibrium, we have

$$\sum F_x = ma_{kx} \qquad ma_{kx} = R_{kx} + R_{ax} \tag{3.4}$$

$$\sum Fy = ma_{ky} \qquad ma_{ky} = R_{ky} + R_{ay} - W_s \tag{3.5}$$

and based on moment equilibrium at the knee joint, we have

$$\sum M_{com} = Is_{com}\alpha_s$$

$$NJM_k + NJM_a - R_{kx} \times d1 + R_{ky} \times d2 + R_{ax} \times d3 - R_{ay} \times d4 + W_s \times d5 = Is_{com}\alpha_s \tag{3.6}$$

where d1, d2, d3, d4, and d5 are moment arms applicable to each force element respectively.

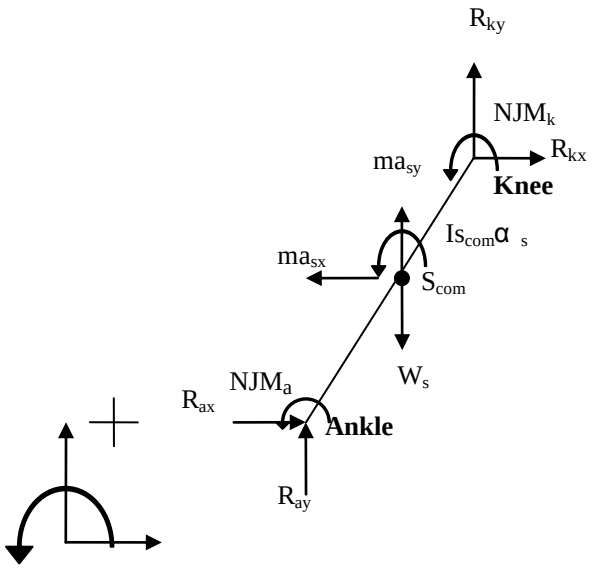

R_{kx}: Horizontal knee reaction force
R_{ky}: Vertical knee reaction force
ma_{sx}: Horizontal mass acceleration of shank
ma_{sy}: Vertical mass acceleration of shank
Is_{com}: Mass inertia of shank
α_s: Angular acceleration of shank
S_{com}: Center of mass of shank
NJM_k: Net joint moment of knee

Figure 4: Free-body diagram of the knee joint and ankle joint

(3) The dynamics of knee-thigh-hip segment

From figure 5, based on force equilibrium, we have

$$\sum F_x = ma_{tx} \qquad ma_{tx} = R_{hx} + R_{kx} \tag{3.7}$$

$$\sum Fy = ma_{ty} \qquad ma_{ty} = R_{hy} + R_{ky} - W_t \tag{3.8}$$

and utilizing moment equilibrium at the hip joint, we have

$$\sum M_{com} = It_{com}\alpha_s$$

$$NJM_k + NJM_a - R_{hx} \times d1 + R_{hy} \times d2 + R_{kx} \times d3 - R_{ky} \times d4 + W_t \times d5 = It_{com}\alpha_s \tag{3.9}$$

where d1, d2, d3, d4, and d5 are moment arms applicable to each force element respectively.

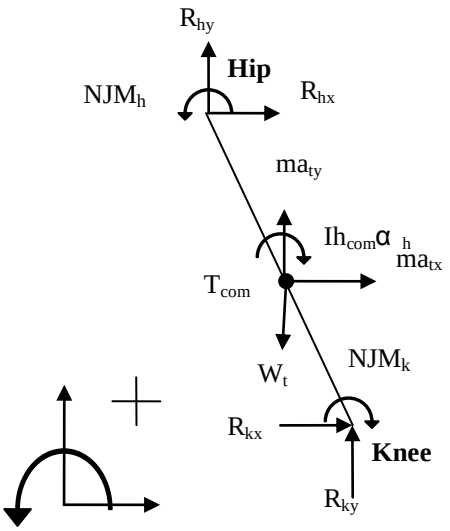

R_{hx}: Horizontal hip reaction force
R_{hy}: Vertical hip reaction force
ma_{tx}: Horizontal mass acceleration of thigh
ma_{ty}: Vertical mass acceleration of thigh
It_{com}: Mass inertia of thigh
α_h: Angular acceleration of thigh
T_{com}: Center of mass of thigh
NJM_h: Net joint moment of hip

Figure 5: Free-body diagram of the hip joint and knee joint

Kinematic variables of interest to this study include the ground velocity, the stride length, the stride cadence, the hip, knee, and ankle joint angular displacement, velocity and acceleration. Kinetically, the ankle, knee, and hip moments, and body weight vector are important factors of a patient's gait. Patient height and weight, along with standard anatomical ratios, establish link lengths and masses for the analysis. The average height, weight and, ratios of each segment can be found in Winter's text book (Winter, 2005).

3.3 Obtaining Quantitative Gait Data

Commonly, quantitative gait data is obtained in a series of steps. First anthropometry is used to document segment lengths. Next, kinematic data (displacements, velocities, and accelerations) are collected experimentally. Finally, the kinematic data is used to calculate the joint moments and forces with link-segment modeling (inverse dynamic modeling). Methods to measure kinetic data (forces, moments) directly involve invasive approaches to implant measuring devices into the

human body surgically to measure the required forces. Therefore, it has had limited application.

Methods of measuring gait kinematics have been extensively developed. Older technologies use a goniometer to measure joint angles and an accelerometer to measure the acceleration of points on the limb segments (Gogia et al., 1987). A goniometer is a rotary electrical potentiometer which measures joint angles by measuring voltage changes induced by rotation of the joint angle (Nasseri et al., 2007). An accelerometer is a standard instrument which can measure the inertially induced displacements of an internal element (Godfrey et al., 2008). Although these two measuring devices are relatively inexpensive and the resulting data can be immediately utilized, the testing effort to acquire a useful amount of explicit gait data is significant, and movement can be encumbered by the connections. Today optical techniques have become the dominant method for gait kinematic study (Horn & Schunck, 1981). Optical systems use lightweight reflective markers on the subject, and multiple cameras to record marker position as a function of time. Computer-based image analysis applied frame by frame results in values for the displacement, velocity and acceleration of each marker and, by extension, of the limb point to which the marker is attached. The data are recorded in the absolute spatial reference system of the recording camera system, and are not limited as to the number of makers used. Encumbrance to movement is minimal when using optical systems which further increases the accuracy of the kinematic data. A complete optical system data capture and analysis system can be expensive.

3.4 Available Standard Gait Data

A “Normal” healthy subject’s gait pattern has left/right symmetry with an average walking velocity of 150 cm/s, a cadence of 115 steps/min, and a stride length

of 150 cm (Rose & Gamble, 1994). The range of normal is wide, and extensive data exist in the literature (Whittle, M. W., 1996, & Perry, J., and Burnfield, J. M., 2010). The normative motions and moments of the ankle, knee, and hip joint corresponding to specified percentages of the gait cycle have been explicitly published by Winter (2005). This normative joint motion from Winter will be used as reference to compare to the predictive computer based simulation of the Mauch S-N-S prosthetic knee.

CHAPTER IV

MAUCH KNEE MODEL DEVELOPMENT

4.1 Test Description

The main goal of the work described in this chapter is to create useful test data that can be utilized to identify the dynamic model of the Mauch S-N-S prosthetic knee (Mauch, H. A. 1958 & 1968) (Ton). A previously used "Mauch Gaitmaster Low Profile SNS Jr." (Ossur, Reykjavik, Iceland) knee cylinder was tested on the bench, setting its performance adjustments at various levels. The major components of the Mauch knee are the hydraulic cylinder which contains all of the functioning components, and a frame which includes the knee pivoting axis and attachment points for the cylinder base, cylinder rod, lower pylon and socket. To simplify lab testing, the cylinder was removed from the frame and tested in isolation (MTS 858 Bionix, MTS, Prairie, MN) (Figure 6). As described below, the gait profiles and frame geometry can be used to calculate the appropriate cylinder velocities. The hydraulic cylinder was driven at various kinematic profiles representing gait at fast, normal and slow speeds while measuring force and cylinder position. Multiple regression techniques were then applied to estimate coefficients of dynamic models ("2-phase" and "4-phase", as

described below) of the prosthetic knee based on data from walking at a normal speed. The dynamic equations applied to slow and fast walk data to evaluate the effectiveness of the models.

The past history of this hardware is unknown, but it shows no sign of leaks or abuse and a veteran prosthetics technician (and a Mauch knee-wearing amputee) who examined and judged it to be in normal working condition. The testing machine was programmed to apply the displacements and record the resulting forces. Each of the slow, normal, and fast gait cadence was cycled 5 times to obtain a large set of input-output data pairs. The testing was repeated for different combinations of three values of the manual flexion and extension damping settings and three walking cadences.

Figure 6: Experimental setup of Mauch S-N-S prosthetic knee cylinder on MTS 858 Bionix test system. Within the circle is the hydraulic cylinder of the Mauch S-N-S prosthetic knee.

4.2 Knee Cylinder Experimental Data Generation

To develop a dynamic model, extensive data sets matching input conditions, e.g., hydraulic cylinder displacement trajectories, and output results, e.g., hydraulic

cylinder force trajectories, are required. To ensure that the data collection covered a range of variables relevant to gait, slow, normal, and fast walking data from literature, specifically knee angle trajectories, were used (Winter, 2005). The prosthetic knee geometry (figure 7) was utilized to calculate cylinder position vs. time profiles using these data:

$$\overline{bc} = \overline{ac}^2 + \overline{ab}^2 - 2\overline{ac} \times \overline{ab} \times \cos(\alpha) \quad (4.1)$$

where

$\overline{ac}$: length of the moment arm

$\overline{ab}$: length from center of rotation to bottom pivot point of cylinder

$\overline{bc}$: length of hydraulic cylinder

α: angle between $\overline{ac}$ & $\overline{ab}$ and α = knee angle + 90°

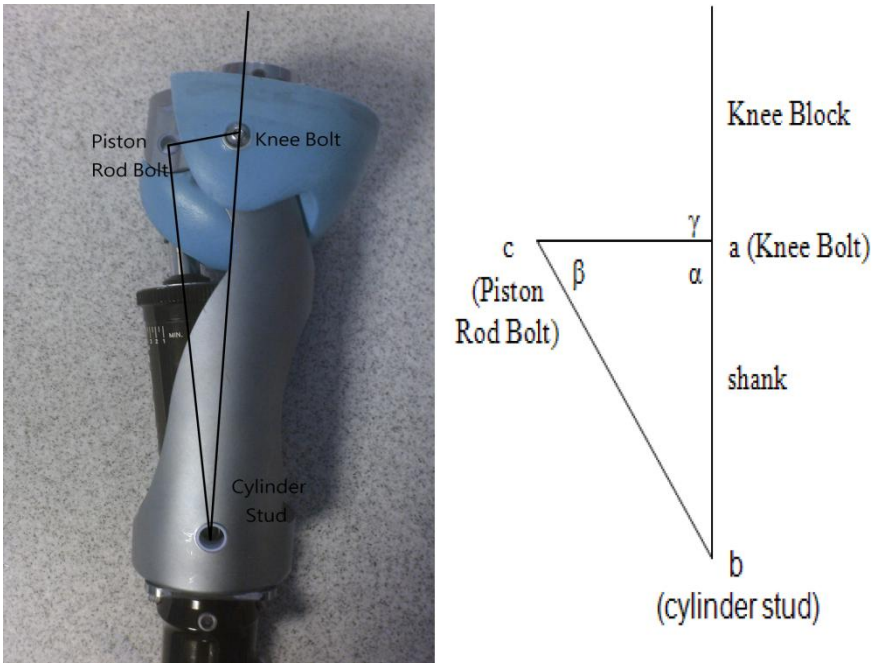

Figure 7: General geometry of the prosthetic knee

The knee angle profiles (Figure 8, top left) of slow, normal, and fast cadences and later the calculated cylinder displacement profiles (Figure 8, bottom right) were modified to capture the hyperextension operating mode of the Mauch Knee (as

described in chapter II). The minimum knee angle during stance phase of the original knee angle profiles was shifted to zero such that it enters the hyperextension mode while the total angular displacement to the peak angle of stance and swing phase remain the same. Then conversion of the angular knee motion to linear motion of the cylinder was made using Eq. 1 and the adjacent 4 points of the minimum knee angle during stance phase were also made equal to the value of the minimum knee angle (0 degree) to ensure sufficient duration. The testing setup applied the time history of piston displacements while recording the resulting forces. Each test condition was cycled 5 times and the data were collected at 361.4 Hz which ensured that more than 300 data points for a single gait cycle were obtained. The testing was repeated for different combinations of three dial values, specifically 0, 90, and 180, of the manual flexion and extension damping settings; and three walking cadences, specifically slow, normal, and fast. A total of 9 nine dial conditions for 3 walking speeds resulted in 27 test conditions.

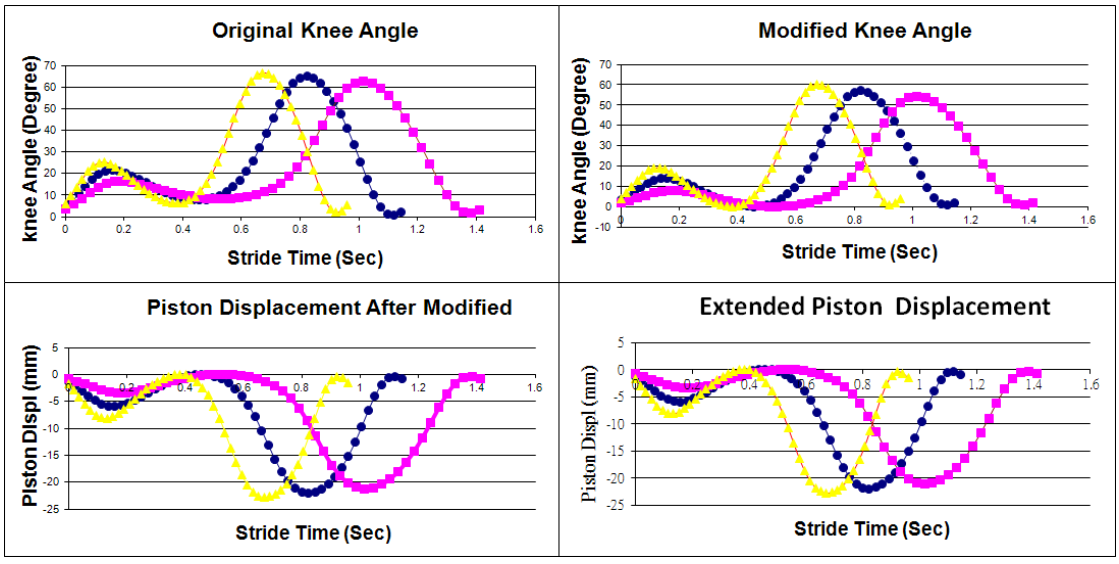

Figure 8: Original knee angle data (left top), modified knee angle data (right top), vertical displacement of the piston relative to modified gait data (left bottom), vertical displacement of the piston with extended period of time during the end of stance phase to insure the switch of stance control to swing control (right bottom). Triangular: fast gait, circle: normal gait, and square: slow gait.

4.3 Model Development

Two dynamics models (Figure 9), at varying fidelities, were developed utilizing the Mauch knee hydraulic piston data and based on the knowledge of the Mauch knee mechanism:

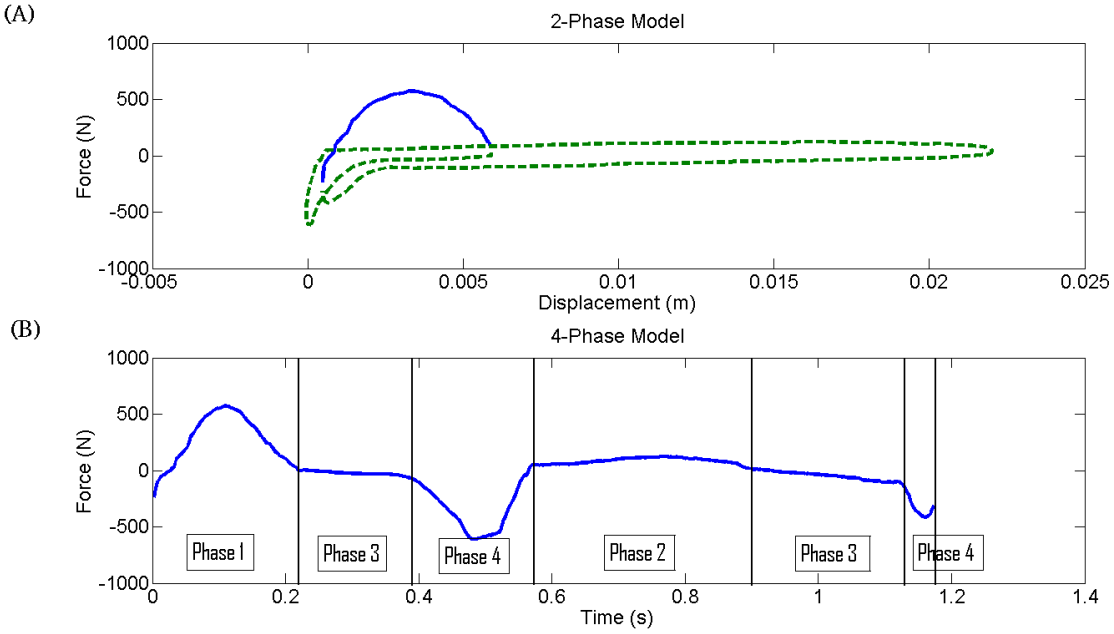

Figure 9: (A): 2-phase model. The solid line, the high force area, where small displacement requires high force to excite the piston, and the low force area, the dashed line, where large displacement requires low force to excite the piston. (B): 4-phase model. Phase 1: Knee flexion in early stance phase. Phase 2: Knee flexion in end stance and early swing phase. Phase 3: Knee extension in stance and swing phase. Phase 4: Hyperextension mode.

(1) 2-phase model (Figure 9-A): This model was a simplified representation of the hydraulic cylinder of the Mauch S-N-S prosthetic knee system. Force-displacement response of the Mauch knee cylinder suggests two dominant phases: Phase 1, the high force section at knee flexion during stance phase; Phase 2, the low force section in all other gait phases except knee flexion during stance phase. The governing force equation of the piston (F_{pis}) of the 2-phase model was written as:

$$F_{pis} = (1 - S_3)(c_1\dot{x} + k_1 x + f_1) + S_3(c_2\dot{x} + k_2 + f_2) \quad (4.2)$$

where x (m) and $\dot{x}$ (m/s) are the piston position and velocity, respectively, $c_{1\text{-}2}$ (N•S/m), $k_{1\text{-}2}$ (N/m) ,and $f_{1\text{-}2}$ (N) are the coefficients of the dynamic equation to be determined for each phase. *S3* is a phase switch variable (Eq. 4.3) which is determined by other two phase switch variables S_1 and S_2. S_1 establishes the extension/flexion state of the knee (Eq. 4.4) from the knee angle velocity. S_2 indicates whether or not the knee has been in the hyperextension state (Eq. 4.5& 4.6).

$$S_3 = 1 - S_1(1 - S_2) \tag{4.3}$$

$$S_1 = 0.5 + 0.5\tanh(\frac{\dot{x}}{x_0}) \tag{4.4}$$

where x_0 is a variable which determines how fast S_1 goes to the extreme values, 0.05 has been empirically verified for our study to provide a fast phase switch of the S_1 value while maintaining reasonable linearity of the equation. S_2 relates to the release and rotation of the balance wheel, after the piston of the hydraulic system passes the hyperextension position, the value of S2 switches until next knee flexion.

$$S_2 = \int \dot{S}_2 ds \tag{4.5}$$

$$\dot{S}_2 = k \times (1 - S_1) \times (0.5 - 0.5\tanh(\frac{x - x_{hy}}{x_0})) - S_2 \tag{4.6}$$

where x_{hy} is the hyperextension position of the piston determined experimentally to be 0.005 cm, and k is another constant controlling the rate at which the parameter changes, 10000 for our study, again, empirically verified, providing a fast phase switch of the S_2 value while maintaining a reasonable linearity for the equation.

Figure 11 shows how the values of S_1 and S_2 change, producing S_3.

(2) 4-phase model (Figure 9-B): This is a more complex model of the hydraulic cylinder in the Mauch S-N-S prosthetic knee system, which takes into account the mechanical design of the knee as well as the test data. As constructed, the Mauch

knee operates in different phases during close-to-normal gait patterns in order to provide appropriate damping resistance: Phase 1 represents the knee flexion in early stance phase, where high resistance prevents knee collapse; Phase 2 represents knee flexion at end stance and early swing, where the resistance is at moderate level; Phase 3 represents the knee extension in both stance and swing phase, where low resistance eases knee extension; Phase 4 represents the hyperextension mode. The governing force equation of the piston of the 4-phase model is:

$$F_{pis} = F_1 + F_2 + F_3 + F_4 \tag{4.7}$$

where F_1, F_2, F_3, and F_4 are the force equations of phases 1, 2, 3, and 4, respectively :

$$F_1 = S_4(c_1\dot{x} + k_1 x + f_1) \tag{4.8}$$

$$F_2 = S_5(c_2\dot{x} + k_2 x + f_2) \tag{4.9}$$

$$F_3 = S_6(c_3\dot{x} + k_3 x + f_3) \tag{4.10}$$

$$F_4 = S_7(c_4\dot{x} + k_4 x + f_4) \tag{4.11}$$

where $c_{1\text{-}4}$, $k_{1\text{-}4}$, and $f_{1\text{-}4}$ are the relative coefficients of each phase equation to be identified. S_4, S_5, S_6, and S_7 are phase switch variables, which dictate the utilization of a specific equation. Like the 2-phase model, these switches are functions of the flexion/extension state, the initiation of the hyperextension state, and the continued presence of hyperextension. Useful values of the four operators can be developed using the previous equations for S_1 and S_2, along with a new term, S_8 phase switch variable, which establishes the initiation of the hyperextension mode:

$$S_4 = S_1 \times (1 - S_2) \times S_8 \tag{4.12}$$

$$S_5 = (1 - S_1) \times S_8 \tag{4.13}$$

$$S_6 = S_1 \times S_2 \times S_8 \tag{4.14}$$

$$S_7 = 1 - S_8 \tag{4.15}$$

$$S_8 = 0.5 + 0.5\tanh(\frac{x - x_{hy}}{x_0}) \tag{4.16}$$

Figure 10 also illustrates the function of these switch variables during gait at normal walking speed.

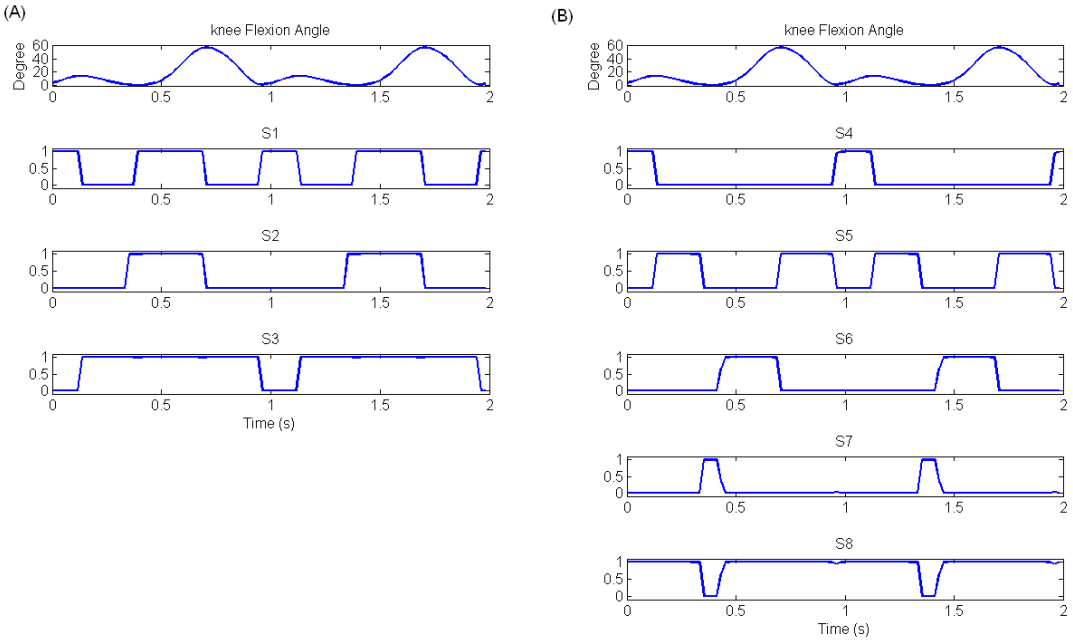

Figure 10: Illustration of the switch variables. (A): Phase switch variables, S_1 to S_3, values of the 2-phase model during the modified normal gait pattern. (B) Phase switch variables, S_4 to S_8 among with S_1 and S_2 in 2-phase mode, values of the 4-phase model during the modified normal gait pattern.

4.4 Extraction of Equation Coefficients from the Data

Given the kinetic-kinematic response of the Mauch Knee hydraulic cylinder, the data were divided into groups to represent each phase based on the switch variables. Then a data fitting approach, multiple regression in Matlab, was used to calculate the coefficients in force equations (*c*, *k*, and *f*) for different phases of the 2-phase and 4-phase models. These coefficients minimized the difference between

predicted cylinder forces and those that were measured. Only the normal walking data were used for data fitting and the process was repeated for each of the Mauch Knee adjustment settings (as prescribed by the dials). In each testing data, one complete gait cycle, starts with heel strike and ends before the second heel strike, was used for data fitting.

Following the determination of model coefficients, the performance of the dynamic models were tested against slow and fast walk data. The adequacy of data fit and models performance for different data sets were established by calculating maximum error (*ME*), root-mean-square error (*RMSE*) and coefficient of determination (R^2) between measured and predicted cylinder force.

(1) maximum error (ME) of the measured and estimated output force:

$$ME = \max(abs(f_m - f_e)) \tag{4.17}$$

where f_m is the measured force and f_e is the estimated force

(2) Root mean square error (RMSE) of the measured and estimated output force:

$$RMSE = \sqrt{\frac{(\sum_{i=1}^{n}(f_{m,i} - f_{e,i}))^2}{n}} \tag{4.18}$$

(3) The square of correlation (R^2) of the measured and estimated output force:

$$R^2 = 1 - \frac{SS_{resid}}{SS_{total}} \tag{4.19}$$

where SS_{resid} is the sum of the squared residuals from the regression and is calculated as:

$$SS_{resid} = \sum_i (y_i - f_i)^2 \tag{4.20}$$

SS_{total} is the sum of the squared differences from the mean of the dependent variable (total sum of squares) and is calculated as:

$$SS_{total} = \sum_i (y_i - \bar{y})^2 \tag{4.21}$$

where

$$\bar{y} = \frac{1}{n}\sum_1^n y_i \tag{4.22}$$

Both SS_{resid} and SS_{total} are positive scalars.

Coefficients for the 2-phase and the 4-phase models obtained from normal walking data are provided in Table 1 & 2. Fit errors for these models and performance of the model for the same dial setting at different walking speeds are summarized in Table 3 & 4. Comparing the R^2 of both models for different gait patterns indicates that the worst model prediction occurs from slow gait with the 2-phase model.

Predicted forces for dial setting F90E90, with 2-phase and 4-phase models, are shown in Figure 11, while the results for the rest of the dial settings are listed in appendix A. Generally, the more complex 4-phase model did better than the 2-phase model when compared to experimental data. Slow gait predicted force data had the poorest model performance when compared to its experimental data.

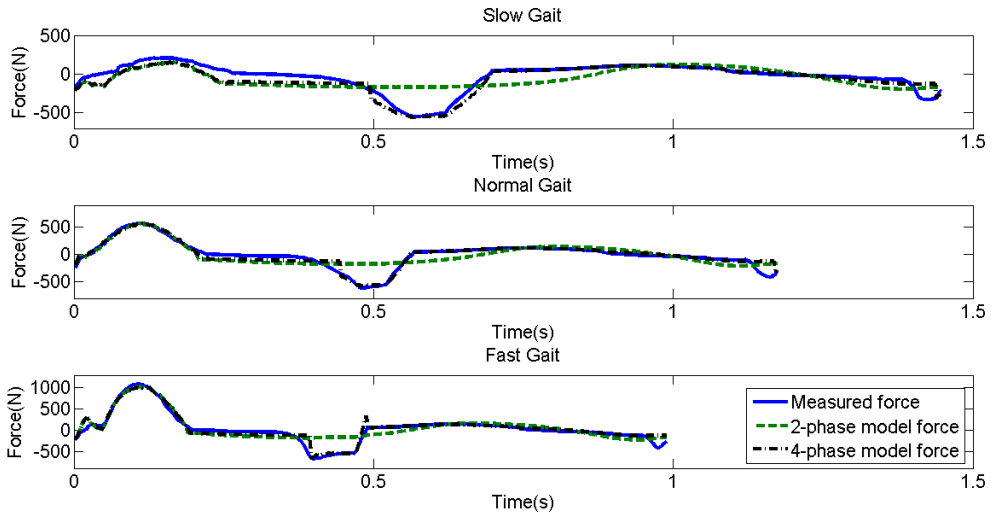

Figure 11: Comparison of measured force with 2-phase and 4-phase model of slow, normal, and fast walking cadences at damping setting of F0E0. Solid line: Measured force, dashed line: 2-phase model, and dash-dotted line: 4-phase model.

Table 1:
Identified Parameters of the 2-Phase Model

Damping setting	Coefficients	Low force section	High force section
F0E0	*f* (N)	-167.21	-241.99
	k (N/m)	12561.98	26295.64
	c (N•S/m)	872.37	16984.52
F0E90	*f* (N)	-219.59	-238.14
	k (N/m)	17537.99	30922.58
	c (N•S/m)	1194.27	17887.49
F0E180	*f* (N)	-308.15	-268.51
	k (N/m)	17497.83	32298.22
	c (N•S/m)	2702.04	18106.59
F90E0	*f* (N)	-165.80	-243.17
	k (N/m)	13648.18	26701.53
	c (N•S/m)	1164.20	17451.44
F90E90	*f* (N)	-189.91	-260.12
	k (N/m)	14115.95	28598.98
	c (N•S/m)	1415.05	17738.71
F90E180	*f* (N)	-276.79	-287.36
	k (N/m)	16293.40	33718.59
	c (N•S/m)	3073.47	19095.22
F180E0	*f* (N)	-136.86	-237.04
	k (N/m)	20985.68	27602.33
	c (N•S/m)	2805.30	19250.65
F180E90	*f* (N)	-191.38	-282.21
	k (N/m)	21798.79	38586.78
	c (N•S/m)	2997.12	20120.11
F180E180	*f* (N)	-213.85	-350.15
	k (N/m)	18745.24	59296.93
	c (N•S/m)	5318.22	23788.67

Note: F represents flexion and E represents extension. The larger the number of the damping setting the higher of the damping resistance. That is, 0 is the lowest damping setting and 180 is the highest damping setting.

Table 2
Identified Parameters of the 4 Phase Model

Damping setting	Coefficients	Stance flexion	Swing flexion	Extension	Hyperextension
F0E0	*f* (N)	-228.05	26.09	-126.08	-506.00
	k (N/m)	27633.70	1981.32	7614.59	650584.41
	c (N•S/m)	16419.23	552.97	264.38	13365.61
F0E90	*f* (N)	-198.67	63.09	-189.22	-625.34
	k (N/m)	29817.45	2034.56	13106.21	725492.77
	c (N•S/m)	16772.68	604.08	392.21	17655.89
F0E180	*f* (N)	-217.21	50.34	-213.01	-691.08
	k (N/m)	30284.26	2042.07	15782.55	731570.90
	c (N•S/m)	16728.67	681.74	3442.98	21982.31
F90E0	*f* (N)	-228.65	26.71	-149.82	-505.12
	k (N/m)	28084.95	2665.81	8371.65	621069.51
	c (N•S/m)	16859.48	1028.37	111.85	14088.77
F90E90	*f* (N)	-243.72	30.95	-184.50	-488.12
	k (N/m)	29975.26	2489.92	10414.64	563312.94
	c (N•S/m)	17087.85	928.70	501.49	14672.24
F90E180	*f* (N)	-248.29	51.98	-200.04	-642.70
	k (N/m)	33143.78	2525.69	13183.04	705511.28
	c (N•S/m)	17948.54	1294.10	3336.63	20464.16
F180E0	*f* (N)	-225.72	-84.49	-143.03	-538.27
	k (N/m)	29613.68	13755.23	9381.34	673484.56
	c (N•S/m)	18696.50	4375.57	262.88	15144.70
F180E90	*f* (N)	-271.31	-32.78	-226.30	-571.31
	k (N/m)	40090.60	11094.10	12585.52	658589.46
	c (N•S/m)	19625.62	3697.46	452.45	18066.77
F180E180	*f* (N)	-337.91	121.08	-216.46	-591.77
	k (N/m)	61295.08	6326.54	11263.19	612172.93
	c (N•S/m)	23210.53	3810.81	3694.52	20566.51

Note: F represents flexion and E represents extension. The larger the number of the damping setting the higher of the damping resistance. That is, 0 is the lowest damping setting and 180 is the highest damping setting.

Table 3
The Accuracy of the 2-Phase Model

	Fast gait			Normal gait			Slow gait		
Damping setting	ME	RMSE	R^2	ME	RMSE	R^2	ME	RMSE	R^2
F0E0	497.5	150.2	68.2	437.1	132.1	81.5	382.4	134.5	39.9
F0E90	495.9	161.4	63.2	545.7	178.6	80.8	363.2	142.9	45.6
F0E180	642.2	192.3	72.5	580.1	181.6	82.4	482.2	188.5	54.6
F90E0	528.6	160.2	68.4	448.0	139.3	80.6	393.8	140.7	45.2
F90E90	538.5	160.1	71.4	407.0	137.6	82.0	368.0	140.4	49.1
F90E180	595.0	184.1	76.2	535.1	170.2	84.7	445.6	174.4	59.7
F180E0	573.8	200.5	72.9	489.6	171.6	79.9	461.0	173.3	59.7
F180E90	613.0	204.1	74.4	513.0	178.9	81.5	450.2	177.7	60.8
F180E180	641.1	213.9	83.7	526.3	188.6	88.0	444.5	187.7	73.4

Note. F represents flexion and E represents extension. The larger the number of the damping setting the higher the damping resistance. That is, 0 is the lowest damping setting and 180 is the highest damping setting. Units of ME & RMSE are Newtons, and R^2 is in %.

Table 4
The Accuracy of the 4-Phase Model

	Fast gait			Normal gait			Slow gait		
Damping setting	ME	RMSE	R^2	ME	RMSE	R^2	ME	RMSE	R^2
F0E0	469.9	78.1	93.5	288.6	59.9	95.0	204.8	66.9	85.1
F0E90	530.6	111.4	88.8	430.7	98.7	90.9	338.9	95.1	75.9
F0E180	717.9	120.6	91.6	413.7	100.1	93.1	381.9	104.2	86.1
F90E0	494.5	87.0	92.3	322.0	68.9	94.3	282.0	73.0	85.3
F90E90	555.3	100.5	90.8	348.0	78.3	92.9	329.4	81.2	83.0
F90E180	680.1	116.0	92.4	418.6	96.0	93.9	378.2	99.8	86.8
F180E0	532.3	101.8	94.2	349.8	79.3	94.8	305.3	87.5	89.7
F180E90	612.4	120.5	92.6	409.5	96.0	93.6	381.8	102.0	87.1
F180E180	642.8	146.1	94.0	427.8	114.9	94.4	435.3	116.0	89.8

Note. F represents flexion and E represents extension. The larger the number of the damping setting the higher the damping resistance. That is, 0 is the lowest damping setting and 180 is the highest damping setting. Units of ME & RMSE are Newtons, and R^2 is in %.

4.5 Discussion

In this study, dynamic models of the Mauch knee hydraulic cylinder were developed; using normal walking experimental data to identify the coefficients for the models and confirming model predictions against slow and fast walking data. For both models, the maximum error generally occurred in the transition of knee extension to hyperextension in both models. That was attributed to phase switching not being perfectly represented in the models. The inertia and viscous effects create pressure effects that vary the timing of the release of the balance wheel's rotation. The constants k and x_0 in this study were selected empirically to be 0.05 and 10000 to cause a rapid yet continuous phase switch as discontinuities in numerical representation of the Mauch knee system are expected to cause convergence problems for future gait simulation studies. Conceptually, more complex system identification methods (Ljung, 1999) that included these parameters in a full data study might have identified better values to smooth the transitions.

As expected, the 2-phase model had a lower accuracy (Table 2) since certain mechanical aspects of the internal design were not considered. Representation of the high force region, when the internal valve is closed, was more faithful to the data, particularly when tensile forces were developed in the system. The low force region incorporated a variety of conditions including flexion in swing phase, extension and hyperextension without accommodating the differentiation these individual models and therefore the model had lesser accuracy here. The 4-phase model incorporated different operating modes at a finer resolution, including switch parameters to differentiate phase and represent transitional behavior. In return, a more adequate model was obtained, albeit with increased complexity.

Also as expected, the estimated models performed better when compared against the normal gait data from which the model coefficients were derived (Table 2, Figure 7). Performance degraded, particularly for slow gait. Both models assume linear behavior of the mechanism, and slow gait (lower velocity flows) may have more impact from non-linear hydraulic fluid flow effects in the hydraulic cylinder, orifices, and valve at slower flows. Accepting this discrepancy (and associated inaccuracies) creates less complex model equations which the simulation software utilized in the following chapters can process more easily. The 2-phase model is less accurate but simpler than the 4-phase model and may be easier to use as a component of a complex system simulation. Furthermore, it can be observed that the hyperextension mode (phase 4 in 4-phase model) of the system is where the 2-phase model has the largest deviation of force prediction. However, if the hyperextension mode does not occur in the simulation, the predictions of the 2phase model will be much closer to reality.

This analysis applies strictly to a single Mauch knee cylinder. When properly integrated into the geometry of a complete prosthetic knee it may approximate the performance of other Mauch knees of the same type. Mauch cylinders are used with a number of different frame designs and therefore the overall prosthetic joint kinematic-kinetic performance would vary. The dynamic modeling methodology employed was straightforward and effective and can potentially be applied to other Mauch knee samples, or to other artificial knee designs and to other prosthetic components, e.g. at the ankle.

The socket, prosthetic knee and the ankle/foot are all major components of a prosthetic knee which directly affect the functional kinetic and kinematic performance of a prosthetic leg. The characteristics of the ankle/foot have been studied and

analyzed (Lehmann et al., 1993, Strbac & Popovic, 2012, Fey et al., 2013, and Au & Herr, 2008). The socket performance is a difficult modeling issue, because the effects on kinematics and dynamics are very highly impacted by an individual's specific fit issues. (Sanders & Daly, 1993, and Faustini et al., 2006) It should be possible to progress with modeling based on the current state of knowledge, which in turn may lead to improved understanding. In our study, a dynamic model of the Mauch knee, a widely employed prosthetic knee, was developed. The approach outlined in our study can be used for other prosthetic component model development studies. Along the aforementioned data and models, it may be possible to build system level models of a prosthetic leg, incorporating all these components. In future, such models can be utilized to estimate prosthetic leg function for various activities, and to predict the capacity of a given prosthetic leg construction and adjustment to realize a desired gait pattern; all providing new insights for better component understanding, design, selection, integration and improved rehabilitation programs and eliminating the need for exploratory field testing with patients to develop and refine prostheses.

CHAPTER V

MAUCH S-N-S KNEE AMPUTEE GAIT SIMULATION

5.1 Overview

With the human subjects testing approach to prosthetic knee test performance characterization, the range of normal gait patterns is extremely large because of the variability of the subjects. This kind of testing must therefore be very focused on statistical significance and power. In conventional tests of prosthetic leg biomechanical performance, human subject variables (Graham et al., 2007, Schmalz et al., 2002, Sanderson et al., 1997, and Jaegers et al., 1995) such as weight, height, prosthesis fit, experience using a prosthetic leg, tissue contact related issues, pathological history, health condition, prosthetic leg alignment, and musculoskeletal or neurological dysfunction, also have to be taken into account. Isolating prosthetic leg issues from these factors is difficult. However, the evolving technology of musculoskeletal simulation offers a means to unambiguously define and control the conditions external to the prosthetic leg, and determine its performance under the assumed conditions.

The power of modern computer tools has made it possible to perform sophisticated mathematical modeling of gait (Thelen & Anderson, 2006, and Piazza, & Delp, 1996). Musculoskeletal modeling considers the skeletal system as a

system of links and joints, powered by a system of interconnected elastic tendons and actively contracting and relaxing muscles (Seth et al., 2011, & Hoy et al, 1990). These models make it possible to perform dynamic studies of the musculoskeletal system; our model of the prosthetic knee facilitates extensions of the methodology to studies of the amputee.

SIMM Dynamics Pipeline (Musculographics Inc., Chicago) was an early musculoskeletal model program. Opensim is probably the standard in the field now for these simulations (Seth, et al., 2011). This is an evolving open source program, but it currently has not shown good results for determining optimal performance under a given set of conditions because it doesn't handle task constraints well. GaitSym (University of Manchester, Manchester) is a new program which does handle optimization problems, but requires sophisticated hardware and extraordinary amounts of running time to reach a solution. For our study, we selected the simulation software, Gait2D, provided by Orchard Kinetics LLC, Cleveland, OH. It is capable of optimal gait determination, and runs quickly and efficiently on a conventional desktop computer.

5.2 Orchard Kinetics Musculoskeletal Model

As suggested by its name, Gait2D software simulates 2 dimensional gait patterns. Several published reports on its use are available (van den Bogert et al. 2012, and Ackermann, & van den Bogert, , 2010). Gait2D uses implicit methods rather than direct solution of ordinary differential equations (ODE's) (van den Bogert, 2011) to perform numerically efficient calculations of optimal gait patterns. The implicit method, compared to employing ODEs, provides benefits including less simulation time and the capability of predictive simulations. In general, ODEs for musculoskeletal simulation are numerically stiff and highly nonlinear requiring many

small time steps to maintain numerical stability. By using the first order Rosenbrock method (Rosenbrock, 1962/1963), the implicit method is able to mitigate some of the ODE's problems when solving forward dynamic problems while maintaining a low degree of RMS error when running at real-time speed. When applied to predictive gait simulations, Gait2D's implicit method uses a direct collocation to obtain the optimal control solution. However, issues related to convergence of gradient-based solvers are still a considerable numerical challenge to this software. The Mauch knee system model must have continuous derivatives to enable computation of an optimal solution using Gait2D.

Van den Bogert et al. (2011) have described the use of Gait2D to simulate the gait of a healthy subject. The model consists of seven body segments (trunk, and left and right thigh, shank, and foot) and sixteen muscle groups (right, and left of Iliopsoas, Glutei, Hamstrings, Rectus, Vasti, Gastroc, Soleus, and Tibialis Anterior). The body segments have nine kinematic degrees of freedom; global X and Y coordinates of the trunk origin (hip), global orientation of trunk, and right and left hip, knee, and ankle angles. To describe the system dynamics, the nine degrees of freedom of the body segments result in 18 state variables, consisting of the 9 generalized coordinates and 9 generalized velocities. The 16 muscle groups have 32 state variables (muscle activation and contraction for each). These 50 variables results in 50 dynamic equations to simulate the gait of a normal subject. The original body segment lengths and mass properties were calculated from subject mass and height obtained from Winter's textbook (Winter, 2005). Gerritsen et al (1988) provide muscle properties. For convenience, these parameters are listed in Appendix B of this document. The heel-ankle horizontal distance was originally assumed to be 6/180 times of subject height in the simulation software.

In our study, we want to extend the use of Gait2D to predict the best achievable amputee gait with a Mauch knee under certain assumed conditions. This is an optimal control problem, with optimality defined in terms of minimizing both the deviation between normal and amputee gait patterns and the muscle activation energy. These two factors must be weighted in the objective function, to allow the solver to balance deviations in gait with expenditures of energy. The solution is determined by finding the state and control trajectories of the musculoskeletal model, for 0< t < T defining a compete gait cycle, such that, (1) the system equations are satisfied at all times, (2), the state trajectory is perfectly periodic with period T and forward translation of v*T where v is the prescribed walking speed, and (3) the objective function F is minimized. The objective function F which used to solve to optimal control problem is:

$$F = \frac{W_{track}}{11}\left[\frac{1}{N}\sum_{i=1}^{10}\sum_{j=1}^{N}\left(\frac{s_{ij}-m_{ij}}{SD_{ij}}\right)+\left(\frac{s_{dur}-m_{dur}}{SD_{ij}}\right)\right]+\frac{W_{effort}}{16}\sum_{i=1}^{16}\sum_{j=1}^{N}u_{ij}^{E} \qquad (5.1)$$

where

N is the number of time points in the gait cycle

S_{ij} is the simulated value of variable i at time j

m_{ij} is the measured value of variable i at time j (an average of human trials)

SD_{ij} is the between-trial SD of measured variable i at time j. Normalization of the tracking error by SD will ensure that variables that are very reproducible in the subject, will also be tracked more closely.

$_{dur}$ is the duration of the simulated and measured value

W_{track} and W_{effort} are the weights applied to achieving minimal kinematic error and minimal energy consumption. The first term with W_{track} encourages the model to follow 11 gait kinematic variables, (left and right 3 joint angles, left and right horizontal and vertical ground reaction forces, and gait cycle duration) from Winter's

textbook. The second term with W_{effort} encourages the 16 muscle groups in the direction of lower muscle activation. Tthe exponent E=3 was recommended (Crowninshield & Brand, 1981) to make this term equivalent to a measure of fatigue. Values of 1 and 20 of W_{track} and W_{effort} were found experimentally by the developers to provide realistic simulation solutions.

5.3 Knee Model Integration and Solution Generation Issues

To simulate the gait pattern of a transfemoral amputation subject, all ankle muscles (Gastorc, Soleus, Tibialis Anterior) and knee muscles (Vasti, Rectus, Femoris, Hamstrings) of the right leg were removed and replaced by the representative dynamic model of the Mauch knee and a torsional spring representation of the prosthetic ankle in the Gait2D musculoskeletal model. This approach to the prosthesis adds no extra variables to the dynamic system. The insertion of the Mauch knee system requires 4 extra variables, 3 phase switch variables and 1 moment equation due to the piston force, for both 2-phase and 4-phase model. The knee moment relative to the piston force of the hydraulic system can be calculated based on the geometry of the prosthetic knee shown in figure 7. Based on the principal of virtual work, the relationship between hydraulic cylinder force and knee moment is,

$$-M_{knee}\partial\alpha - F_{hy}\partial\overline{bc} = 0 \tag{5.2}$$

where

M_{knee} is the knee moment and F_{hy} is the force of the hydraulic cylinder

Therefore,

$$M_{knee} = -F_{hy}\frac{\partial\overline{bc}}{\partial\alpha} \tag{5.3}$$

where,

$$\overline{bc} = \sqrt{\overline{ac}^2 + \overline{ab}^2 - 2\overline{ac} \times \overline{ab} \times \cos(\alpha)} \tag{5.4}$$

therefore,

$$\frac{\partial \overline{bc}}{\partial \alpha} = \frac{\overline{ac} \times \overline{ab} \times \sin(\alpha)}{\sqrt{\overline{ac}^2 + \overline{ab}^2 - 2\overline{ac} \times \overline{ab} \times \cos(\alpha)}} \tag{5.5}$$

and

$$M_{knee} = -F_{hy} \frac{\overline{ac} \times \overline{ab} \times \sin(\alpha)}{\sqrt{\overline{ac}^2 + \overline{ab}^2 - 2\overline{ac} \times \overline{ab} \times \cos(\alpha)}} \tag{5.6}$$

A current limitation of the Gait2D simulation software is that the mass and geometric properties of the prosthetic and intact leg need to be symmetrical. Therefore, these properties of both lower extremities in the musculoskeletal model in this chapter were derived from the actual properties of the prosthetic leg available to us for testing. The properties of the actual prosthetic leg segment lengths and masses used are listed in table 6. The height and mass of the subject were also adjusted to be consistent with the prosthetic leg. That is, the original total leg length of the average healthy subject described in Winter's textbook (table 5) is 0.9538 cm, but the actual total prosthetic leg length is 0.8722 m which results in a loss of 0.0815 m in subject height. A similar calculation of subject weight loss has also been applied. The linear torsional spring representing the prosthetic foot/ankle, the Ossur Flex foot (Reykjavik, Iceland), has an approximated stiffness of 350 Nm/rad as indicated by the literature (Lehman et al. 1993). The prosthetic knee was represented by the 2-phase model described in chapter IV due to its more linear characteristics as compared to the 4-phase model.

Table 5
Properties of the lower extremities: prosthetic leg

	Mass (m)	Inertia (kg-m^2)	CMx (m)	CMy (m)	Length (m)	Ankle height (m)	Heel-ankle distance (m)
Thigh	3.7195	0.0641	0	-0.1187	0.4064		
Shank	1.3490	0.0193	0	-0.1351	0.3958		
Foot	0.3850	0.0056	0.0768	-0.0351	0.254	0.0702	0.06

Note: Definitions

Inertia: Moment of inertia with respect to center of mass

CMx: X coordinate of center of mass.

CMy: Y coordinate of center of mass.

Table 6
Properties of the lower extremities: Normal leg

	Mass (m)	Inertia (kg-m^2)	CMx (m)	CMy (m)	Length (m)	Ankle height (m)	Heel-ankle distance (m)
Thigh	7.5000	0.1522	0	-0.1910	0.4410		
Shank	3.4875	0.0624	0	-0.1917	0.4428		
Foot	1.0875	0.0184	0.0768	-0.0351	0.2736	0.0702	0.06

Note: Definitions

Note: Definitions and units

Inertia: Moment of inertia with respect to center of mass.

CMx: X coordinate of center of mass.

CMy: Y coordinate of center of mass.

The 4-phase includes one more nonlinear variable, *S8*, which increases the simulation software difficulties converging on an optimal solution. A major advantage of the 4-phase model is that it represents the switching function at hyperextension, better predicting the resulting cylinder performance. However, as later results will show, the assumed subject when walking "optimally" (best trade-off between kinetics and kinematics) with a Mauch knee equipped prosthetic leg does not trigger this function; therefore the advantage of the 4-phase model over the 2-phase model is significantly diminished because hypertension at the end of stance phase does not occur.

With coding of the extra variables into the system of equations used by Gait2D, simulations with a transfemoral amputation can proceed. A multistep process was used to converge on the ultimate answer: (1) normal gait data from Winter's textbook (2005) was used as the initial parameters to find the optimal solution for a normal subject; (2) this normal solution was used as the initial point to be a transtibial amputation subject gait simulation, (3) finally the transtibial solution was used as a starting point to search for the transfemoral amputation subject gait simulation.

In the transfemoral amputation simulation, due to the natural characteristic of the *tanh* function in the phase switch variables, the value of x_0 determines the switching speed of variables *S1* and *S2*; that is, the smaller the value of x_0 the faster variables *S1* and *S2* goes to the extreme value (-1 and 1 in our case). However, fast responses of the phase switch variables increase the nonlinearity of the *tanh* function which also increases the difficulty of finding the optimal solution. One solution to this issue is to perform a simulation with a large value of x_0 and use the results as a starting point for the next simulation which has smaller value of x_0. This sequence can continue until the model incorporates fast phase switch responses. A value of x_0 less than 0.1 results in phase switch variable values close to either 1 or 0.

5.4 Results

The predicted optimal gait of a transfemoral amputee subject employing a Mauch S-N-S knee system while walking on a level surface has been determined through Gait2D simulations utilizing the 2-phase knee model. The subject walking speed was 1.002 m/s with 1.382 sec per gait cycle. Slow walk is the condition where the 2-phase cylinder model represented the actual hardware least well, making it a useful evaluation case; additionally, as will later be discussed, our experimental evaluation test hardware was not able to function above a slow walk. This simulation

assumed that (1) the prosthetic ankle has a torsional stiffness of 350 Nm/rad (2) the prosthetic knee damping adjustments were set at F0E0, (3) the socket of the prosthesis is perfectly aligned with no relative skin-socket motions, (4) the remaining muscles of the prosthetic side functioned identically to their equivalents on the intact side, and (5) the masses and lengths of segments of the prosthetic and intact leg are identical, with other musculoskeletal parameters also adjusted as described in the previous chapter; (6) the subject does not tend to lean to the intact side more than to the prosthetic side, (7) the ground stiffness is 20000 N/m: and, (8) the weighting in the objective function for kinematic deviations and for muscular effort 1:20 to balance between the goals of minimizing gait pattern deviations and energy consumption.

Figure 12 shows a stick figure representation of the theoretical optimal gait pattern of the subject walking along a level surface with the Mauch S-N-S knee prosthetic leg. The red stick represents the intact leg and the blue stick represents the prosthetic leg. Figure 13 shows the simulated joint kinetics and kinematics of the lower extremities, ground reaction forces (GRFs), muscle activities, and responses of phase switch variables, *S1*, *S2*, and *S3*, of the Mauch S-N-S knee system. In the subplots of the joint angles, the red and blue bands represent the range of normal from Winter's data. The time axis for all the left (intact) leg variables is shifted 50 compared to the left (prosthetic) leg.

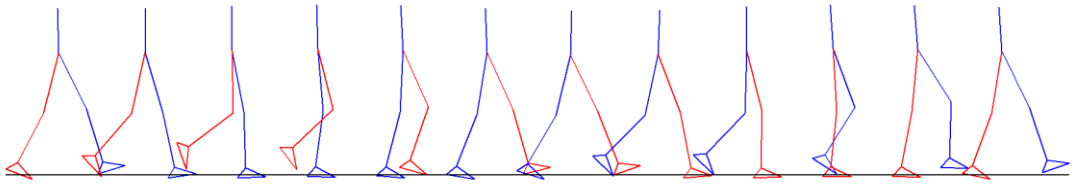

Figure 12: Stick figure of potential optimal gait of subject wearing Mauch S-N-S prosthetic walking on a flat ground. The blue line represents the right (prosthetic) leg,

and the red line represents the sound leg. The Mauch knee damping setting: F0E0. The torsion ankle stiffness: 350 Nm/rad. Gait speed: slow.

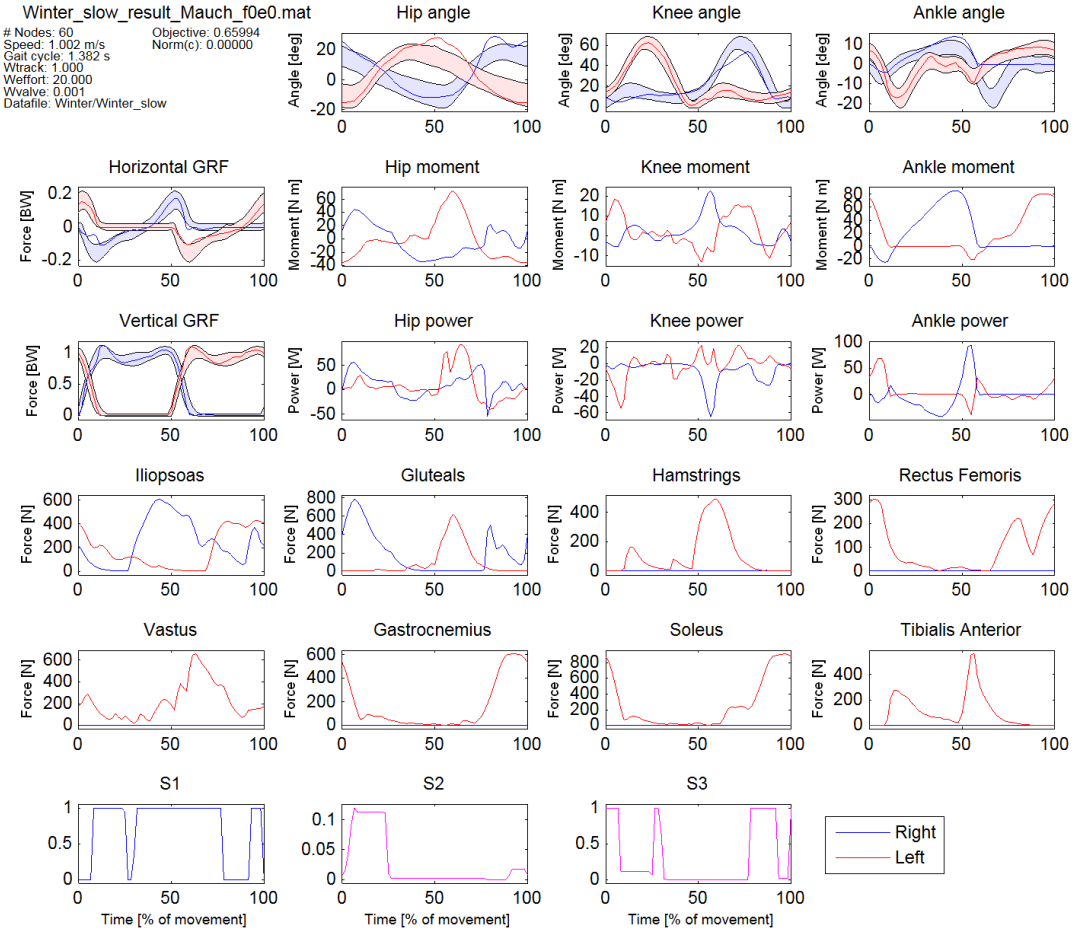

Figure 13: Kinetics and kinematics simulation results of transfemoral amputation patient wearing Mauch S-N-S prosthetic knee. The blue line represents the right (prosthetic) leg, and the red line represents the sound leg. The Mauch knee damping setting: F0E0. The torsion ankle stiffness: 350 Nm/rad. Gait speed: slow.

5.5 Discussion

The results of optimal gait pattern simulation for an amputee patient wearing a prosthetic leg incorporating the Mauch S-N-S prosthetic knee and a prosthetic foot with a stiffness of 350 Nm/rad have been obtained under certain hypothesized physical and physiological conditions as described above. The methodology has proven to be practical to execute. Simulations of this type have a significant potential

to help manufacturers understand how different prosthetic leg components and systems could function under different conditions, and to sort out the major factors affecting those functions. Prosthetists may also find help in simulations developing a prosthesis prescription and set up for particular patients and conditions.

Under the conditions of this simulation, it was found that a subject attempting to walk optimally, as defined for this simulation, will not trigger the unnatural hyperextension condition that is a defining feature of the Mauch design. The minimum knee extension after mid-stance phase did not go below the hyperextension position. Therefore the low prosthetic knee flexion resistance during swing phase will not be obtained. The results may suggest that patients do not need this feature to walk in an energy-efficient and close-to-normal gait pattern with a hydraulic knee such as the Mauch S-N-S design. As noted earlier, with the absence of the hyperextension mode, the accuracy of the 2-phase model does not differ greatly from the 4-phase model. Figure 14, compares the predicted knee moments of both models. The results show only slight differences between the predicted knee moments of the two models. One possibility is that the switching into the designed swing mode at end stance was not triggered is that the required force/energy from the residual muscles to extend the knee and trigger the hyperextension mode was greater than the energy saved by lower resistance during extension. The prosthetic knee system itself does not provide or reserve the required force during knee flexion, and only insignificant knee extension occurs after the mid-stance phase. Different weightings between gait pattern tracking and energy expenditure conceivably could also affect this result.

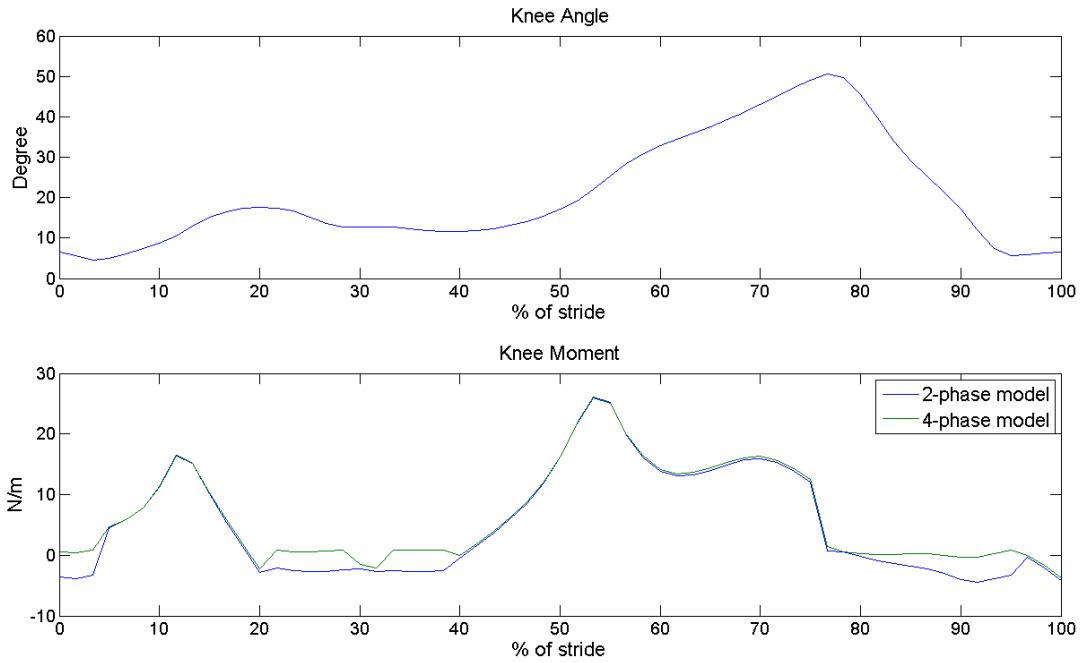

Figure 14: Comparison of knee moments from 2-phase and 4-phase model (bottom) based on knee joint angular motion from 2-phase model simulation result (top).

The assumptions of the physical and physiological conditions due to current software limitations limit the ability of the software to fully model the clinical situation. the currently unavoidable assumptions that the masses and mass distribution of the intact and prosthetic leg are identical, that the residual muscles on the prosthetic side function the same as their equivalent muscle on the sound side, and that the subject gait be two-dimensional, without favoring one or the other side are major discrepancies with respect to reality. The limb masses and mass distribution indeed impact the characteristics of gait motion (Drills et al., 1694) and a higher normal hip flexor moment on the prosthetic limb has been reported (Blumentritt et al, 1998). However this study does define a baseline potential optimal gait of an idealized subject, and provides a basis for follow-on, more refined models that explicate the impacts of the factors concerned.

Ground reaction force was evaluated as an input to the simulation, and was found to be a significant factor. This parameter should be matched in computational

and experimental studies to acquire meaningful testing results. The ground stiffness usually is not particularly mentioned in the published patient test data. A particular patient's environment could make a difference in the performance of a particular prosthetic leg prescription and set-up.

CHAPTER VI

EXPERIMENTAL VALIDATION

6.1 Overview of Possible Experimental Methods and Limitations/Advantage

"How well does the simulation represent the actual event?" is now the issue we want to address. To validate the result of the simulation on human subjects would be very time consuming, expensive and subject to large uncertainties for the reasons already discussed in Chapter V. We proposed to utilize a robotic simulator which will reproduce the hip motion from the simulation result. The assumption of a "perfect" socket interface can also be duplicated. The response of the knee component, the Mauch knee, can be determined and compared to the simulation result.

A leg prosthesis robotic simulator has been built by Richter et al. (2012) at Cleveland State University. The 2-dimentional robotic simulator simulates the x and z plane motion of the gait with 3 degrees of freedom, the vertical hip displacement, the rotational thigh displacement, and the relative translational displacement of the subject and ground. These degrees of freedom are provided by a ballscrew-driven vertical slide coupled to a DC motor, a brushless DC motor and gearbox carried by the vertical slide, and a treadmill respectively. This robotic simulator is capable of a maximum hip vertical displacement of 100 mm with a maximum vertical plane

velocity of 1 m/s., 150 degree of thigh angular displacement with a maximum torque of 75 Nm, and the vertical force capacity is 1200 N.

The treadmill surface is a steel plate covered by a thin moving rubber belt. We made approximate measurements of this ground stiffness by pressing the leg into the belt with measured forces and measuring the displacement of the heel into the rubber with a scale. We obtained approximate values in the range from 400,000 to 580,000 N/m. Clearly the treadmill falls into the range of very stiff ground, where our prior simulation study of this effect indicates that no great precision in the value is required to obtain useful test results.

Real time control of the robotic system is implemented using a dSPACE DS-1102 system and associated software (dSPACE, Paderborn) which has been converted to Matlab/Simulink operating interface code for users to enter inputs. An independent Sliding Mode Control algorithm is used, which provides good robustness properties and straightforward implementation (Edwards, and Spurgeon,, 1998, & Utkin, 1992).

For the validation test, we mounted the prosthetic leg to a flange on the rotational system and used the vertical displacement of the hip, thigh angle rotation, and the walking speed from the gait simulation as test inputs to drive the prosthetic leg. The recorded knee joint motion and moment, the ankle moment, and GRF are then compared to the simulation results.

There are a few limitations of the present robot:

(1) The vertical displacement, velocity, and acceleration change rates of the hip motion are limited to 0.2095 m/s, 3.1853 m/s^2, and 42.1258 m/s^3 respectively, and therefore the robot is limited to a slow walk condition; furthermore, a smooth algorithm which creates a polynomial representation

of the test data (figure 15) was used to eliminate a sharp change rate of the vertical movement when they hits the limit.

(2) The treadmill speed increments are limited to about 0.16 km/min, which makes it impossible to exactly duplicate the standard slow walking speed.

(3) The vertical force limitation of the robot will cause a test shutdown if the hip vertical motion profile is derived from a simulation with softer ground than provided by the robot. A "soft" simulation penetrates the ground more and therefore has greater hip vertical displacement. The treadmill as presently configured simply won't compress enough to allow the displacement with acceptable force. Most of our simulations in this research were performed with a ground stiffness of 20,000 N/m, but we also have performed additional simulations with ground stiffnesses covering a reasonable range of possibilities, including the range of the treadmill stiffness for the purpose of robotic simulation.

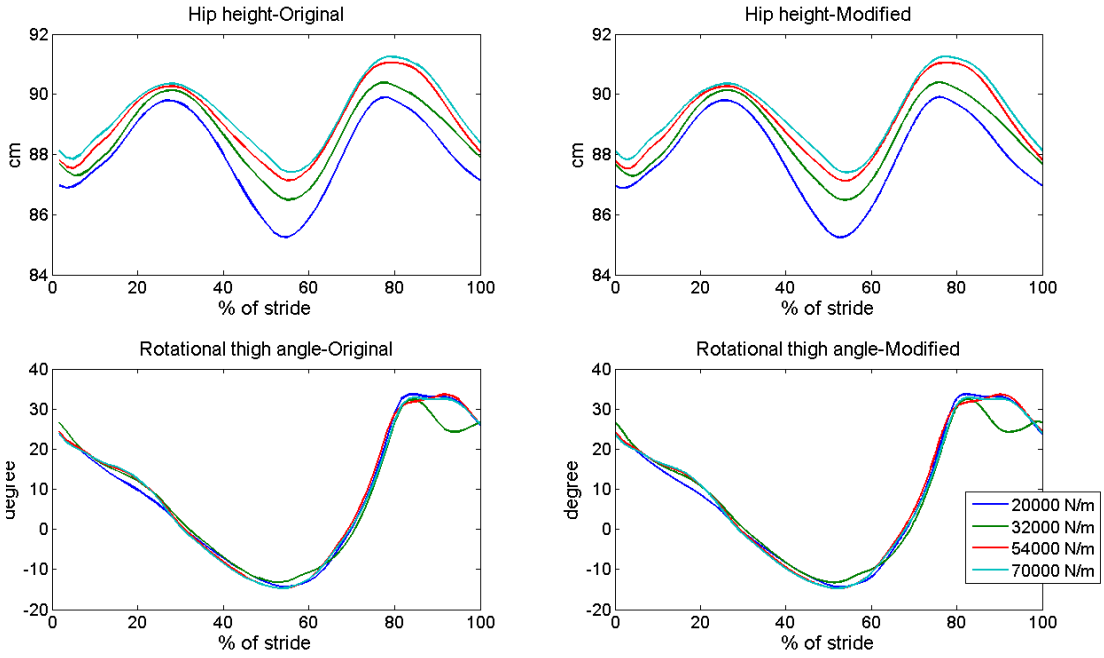

Figure 15: Comparison of original and modified test inputs. Left: Original hip height and rotational thigh angle. Right: Modified hip height and rotational thigh angle.

6.2 Validation of Our Model

In most simulations, the foot-ground interaction generally focuses on generating a reasonable ground reaction force. The natural leg is able to adjust the leg stiffness on different surfaces to maintain similar ground reaction forces (Ferris et al., 1998). Therefore, in most published simulations, the ground stiffness has not been given much attention and has been integrated with the stiffness of the leg. However, for the purpose of robotic simulation of a prosthetic leg, the stiffness of the ground plays an important role because the leg components are almost infinitely stiff axially and there is no pelvis to rotate, further reducing the apparent stiffness.

With soft ground, the toe and heel will 'penetrate' the ground to moderate ground reaction force and also increase vertical displacement. Without significant additional development, this amount of penetration may never be achieved when testing on the treadmill. What behavior to assume computationally/experimentally for a prosthetic leg attached to a patient is still an open question.

In our computational simulation, the weights of both intact and prosthetic leg were assumed equal to the prosthetic leg described in chapter 4. The effective relative stiffness of ground/tissue in the simulation was usually assumed to be 20000 N/m which is relatively much softer than the actual value of the contact surface of the treadmill. The penetration depth of the toe and heel into the ground in the simulations at 20000 N/m has a maximum value of 10 cm which is not realistic but is generally accepted as a compensation for not modeling the effects on stiffness of the natural leg and pelvis. We have performed simulations with various ground stiffnesses and compared the kinetic and kinematic performance of the prosthetic leg (figure 16). The results show nearly identical kinetic and kinematic prosthetic leg performance across the range tested. We have simulations with ground stiffness of 20000, 32000, 54000,

and 70000 N/m and used the robotic simulator to evaluate those simulation results. The higher values do not result in attempted vertical displacements/ground penetration that overloads the force capacity of the robot. The vertical displacement of the hip and rotational thigh angles to the ground of the simulations are shown in figure 17.

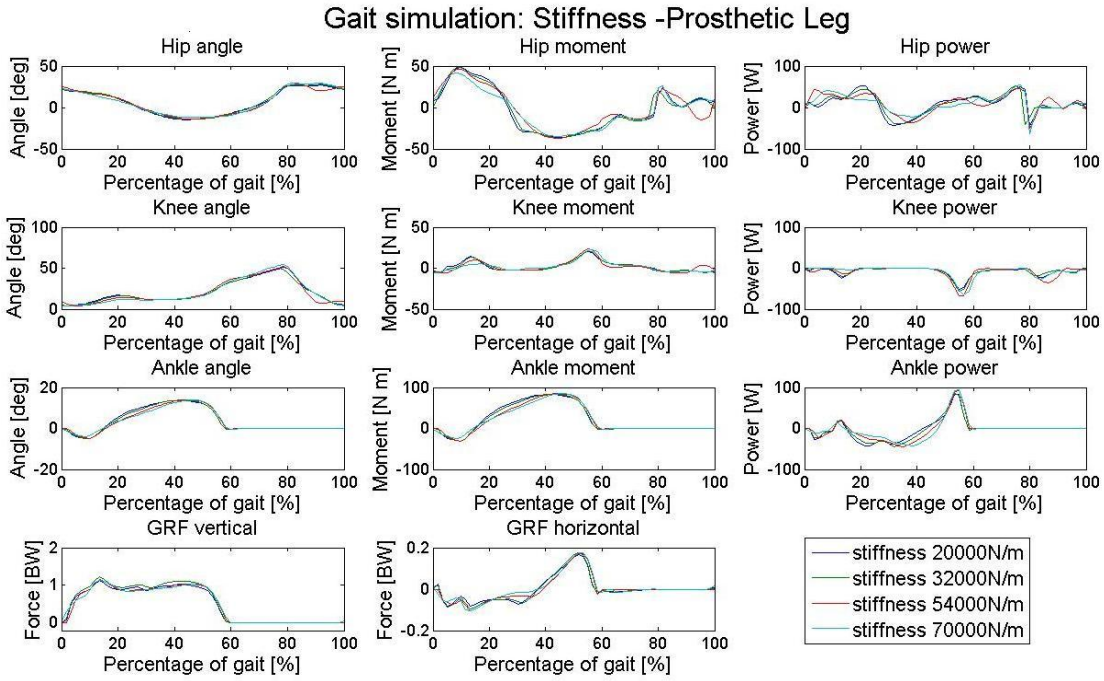

Figure 16: The kinetic and kinematic performance of the prosthetic leg with ground stiffness of 20000, 32000, 54000, and 70000 N/m

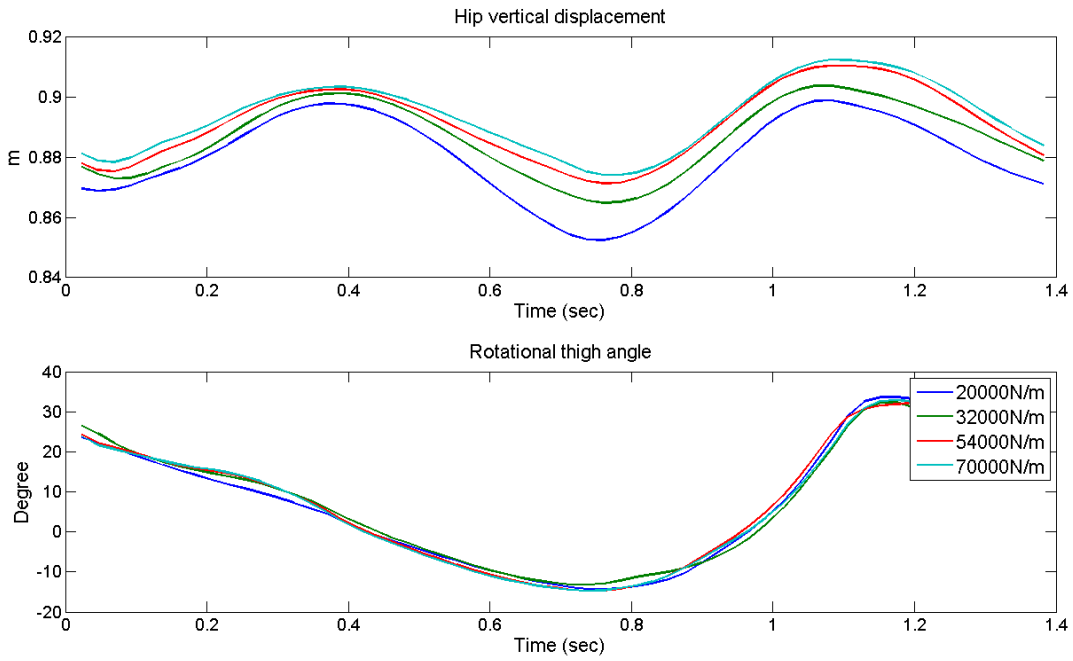

Figure 17: Robotic test inputs. Top: the vertical displacements of the hip. Bottom: the rotational thigh angles to the ground. Walking speed is 1.002 m/s.

6.3 Robotic Validation

To validate the computation simulation results, the prosthetic leg was mounted on the robotic simulator as shown in figure 18. The hip vertical displacement, rotational thigh angle, and the walking speed from the computation simulation results (figure 16 & 17) were extracted and programmed into the robotic simulator. The vertical and angular positions were aligned prior to every single test and the knee moment, knee angle, and vertical ground reaction force were recorded to compare to the simulation results.

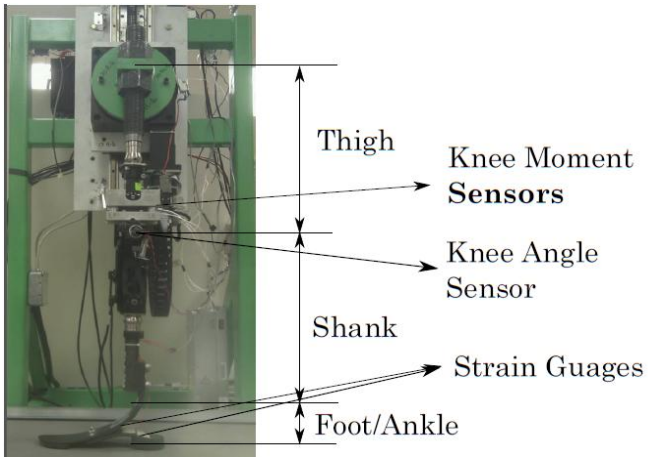

Figure 18: Assembly of the prosthetic leg on the robotic simulator

For our validation, the adjustment of hip displacement was needed due to the discussed ground penetration issue. Two zero positions of the hip displacement with 20,000, 32,000, and 54,000 N/m ground stiffness were used. One created a maximum GRF close to computational simulation results and the other created a maximum GRF close to the limit of robot performance capability.

6.4 Test Results

Figures 19-22 show the comparison of the computational simulation and the robotic test at various foot/ground stiffnesses. In these plots, the blue line represents the simulation results. The red line shows the test results when the simulation hip displacement was used and the robot permitted to hit its force limit. The green line shows test results when the hip motion was adjusted to produce a maximum test ground reaction force similar to the simulation. Figure 22, the test of the 70,000 N/m ground stiffness simulation, only shows the green line because the relevant output did not hit the vertical force limit of the robot.

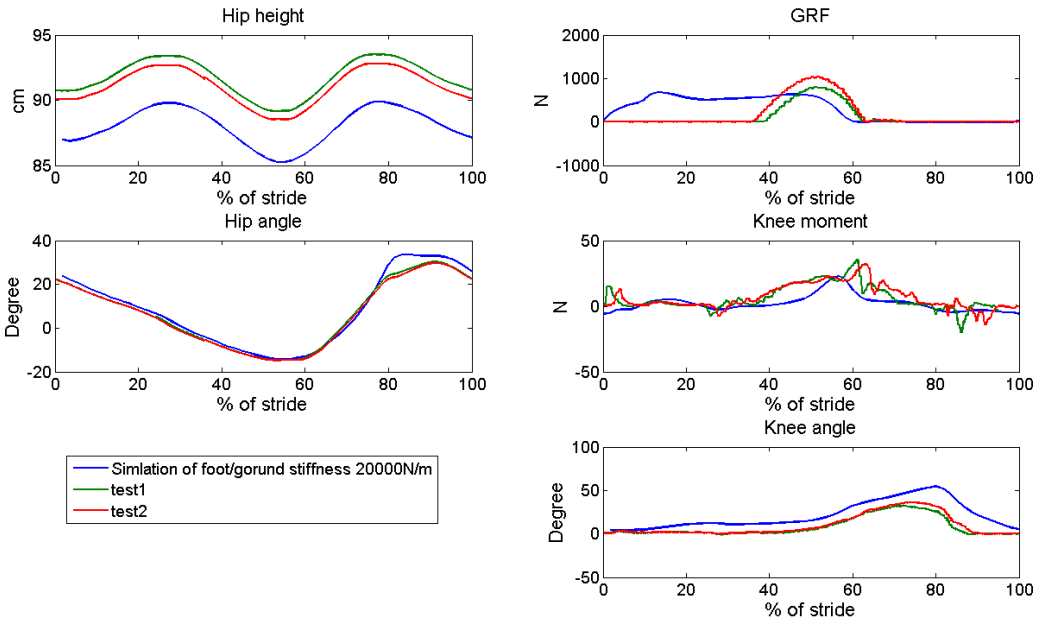

Figure 19: Results of robotic test of simulation with foot/ground stiffness of 20,000 N/m. The blue line represents the results from the musculoskeletal simulation. The green line represents test1 where data was recorded before the maximum GRF hit the vertical force limitation of the robotic system, and the red line represents test2 where data was recorded with the maximum GRF similar to the computation simulation.

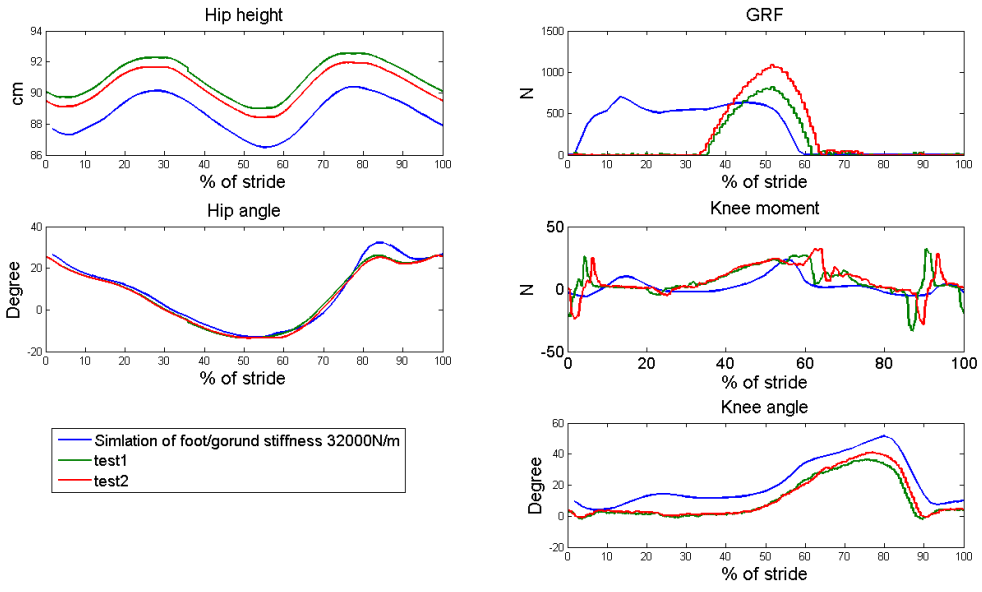

Figure 20: Results of robotic test of simulation with foot/ground stiffness of 32,000 N/m. The blue line represents the results from the musculoskeletal simulation. The green line represents test1 where data was recorded before the maximum GRF hit the vertical force limitation of the robotic system, and the red line represents test2 where data was recorded with the maximum GRF similar to the computation simulation.

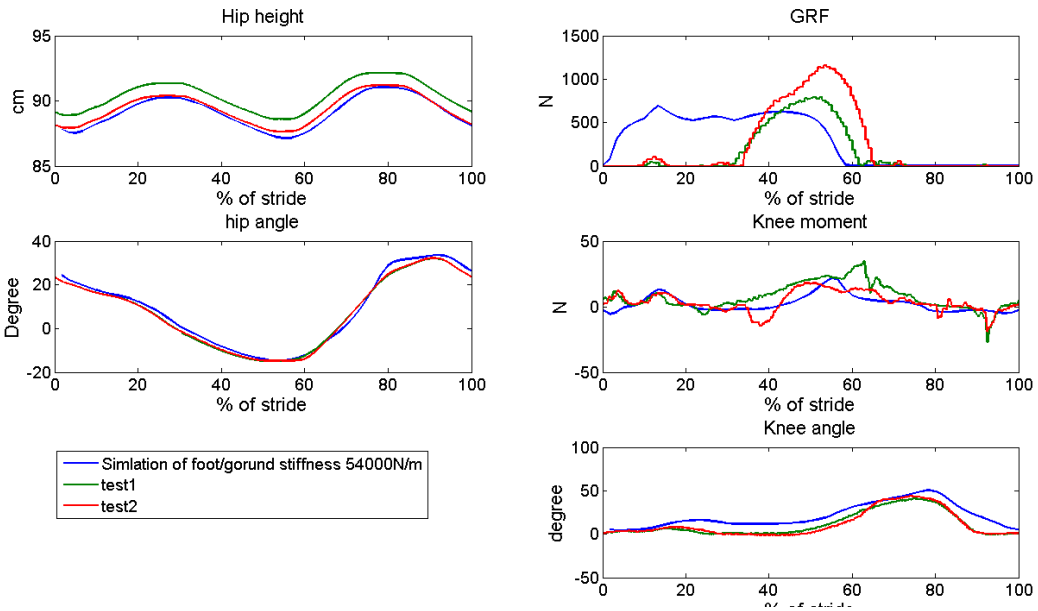

Figure 21: Results of robotic test of simulation with foot/ground stiffness of 54,000 N/m. The blue line represents the results from musculoskeletal simulation. The green line represents test1 where data was recorded before the maximum GRF hit the vertical force limitation of the robotic system, and the red line represents test2 where data was recorded with the maximum GRF similar to the computation simulation.

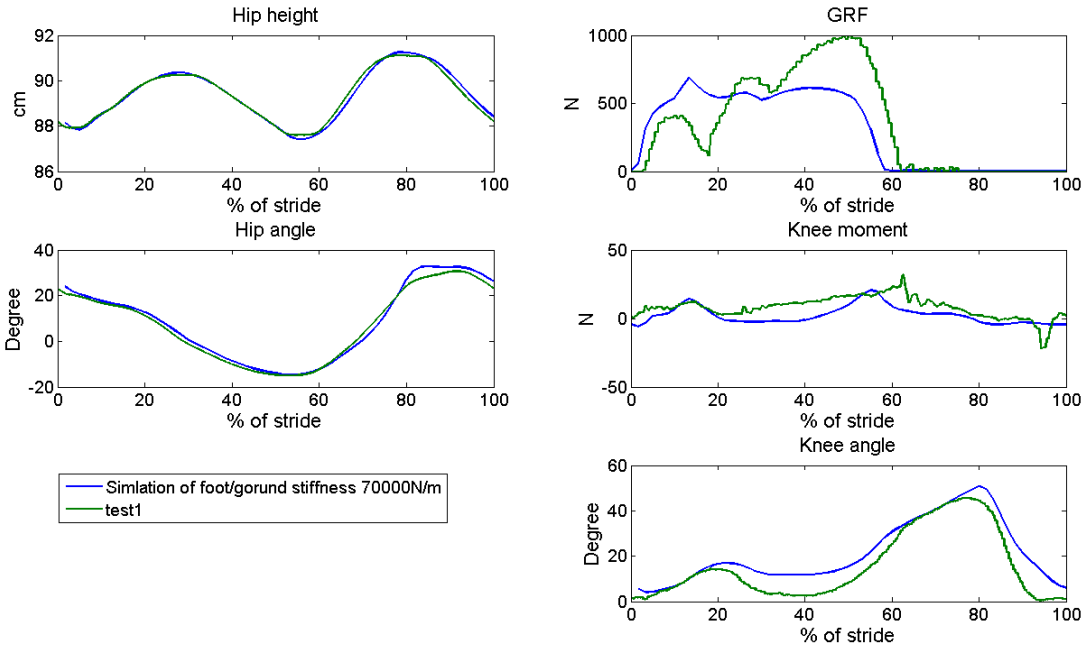

Figure 22: Results of robotic test of simulation with foot/ground stiffness of 70,000 N/m. The blue line represents the results from musculoskeletal simulation. The green line represents test results from the robotic simulation.

6.5 Discussion

These data indicate that the simulation using Gait2D and our 2-phase Mauch knee model and robotic testing of hardware produce similar results when the simulation uses high ground stiffness such as exists with the robot. With stiff ground, the kinematic parameters track each other reasonably well. The pattern of ground reaction forces shows some differences. At 50% stride, the experimental GRF is higher. This may be because the foot/ground stiffness is not perfectly represented by a constant value from heel strike to toe-off. A more complex model for the prosthetic ankle/foot behavior may also make a difference. Given the critical nature of hip height to the value of GRF in the robotic tester, small differences in the set up of the various components of the prosthetic leg as compared to the assumed linkage relationships in the simulation may also make a difference.

6.6 Conclusion

The robotic test and computational simulation approach characterization of a prosthetic leg from fundamentally different directions. That they agree as closely as they do at this early stage of development of both techniques is highly encouraging. The computational study used the less precise 2-phase model to ease numerical convergence and a simplified model of the ankle/foot. Ankle/foot behavior is more complex when the effects of the roll from heel to are considered (Singer et al., 1995). More detailed models of the structure, compliance and mass distribution of the prosthetic leg might result in more accuracy in the simulations. The formulation of Gait2D could also be significantly refined to include the differences between the intact and prosthetic leg; the impact of comparisons to a one legged robot would be interesting to see. The existing robot might be improved with feedback control that enabled optimization of its operating conditions. More force and acceleration/velocity

capability in a new model would be highly valuable, as would an infinitely variable treadmill speed. One could experiment with pads attached to the foot to obtain various levels of ground stiffness. It is fair to say that both the computational and robotic testing approaches show good promise and should be further pursued in the future.

CHAPTER VII

MODEL APPLICATION: KNEE DAMPING AND ANKLE STIFFNESS EFFECT ON GAIT PERFORMANCE

7.1 Overview

In general, the capabilities of lower limb prostheses have been analyzed by gait-lab testing of subjects and generally only the overall gait kinetics and kinematics of subjects with different types of prostheses were compared (Graham et al., 2007, Schmalz et al., 2002, Sanderson et al., 1997, and Jaegers et al., 1995). The effect of intrinsic properties of the prosthetic components, such as the knee damping setting or the ankle stiffness are not easily isolated or evaluated in such programs. The selection of the optimal setting of the prosthetic knee and the most suitable prosthetic ankle/foot principally relies on the subject's personal perceptions and the professional judgment of the prosthetist which considers factors such as the subject's age, weight, level of activities, and lifestyle (Prince et al., 1998, & Micheal, J., 1987). In this chapter we will demonstrate an application of the simulation technique, evaluating the effect of various levels of knee damping and ankle stiffness on the prosthetic leg's ability to produce near normal gait patterns with minimized energy demands from the patient.

The basic functions of a prosthetic foot are (1) weight support during stance phase, (2) shock absorber at heel strike, and (3) simulation of the toe-off dynamics at the end stance phase (Edelstein, 1988). Most ankle/foot prostheses on the market use a passive spring design and the characteristic of the prosthetic ankle/foot system can be approximated by a torsional spring during stance phase; the ankle/foot power during swing phase is negligible (Shamaei et al., 2011). The benefit of using a torsional spring prosthetic foot/ankle model for this project is the simplicity of its highly linear mathematical model which reduces the numerical challenges encountered by the simulation software when converging to a solution for the entire system. Ankle/foot prostheses are not always strictly linear, and more complex models can take into account the changing properties of the hardware as the contact point progresses from heel to toe. There are other devices which are actively powered (Au et al., 2008), or microprocessor controlled (Mitchell et al., 2013). Future simulations of truly optimized prosthetic limb systems will need to account for non-linear behavior in the ankle/foot.

7.2 Method

7.2.1 Musculoskeletal model

In the simulation, a male, unilateral transfemoral amputation patient 180 cm tall and weighing 75 kg was defined as the study subject. The right leg of the subject was "amputated" and replaced by the prosthetic leg. In the musculoskeletal model, the ankle/foot muscles (Gastroc, Soleus, Tibialis Anterior) and knee muscles (Vasti, Rectus Femoris, Hamstrings) of the prosthetic side were removed and replaced by the prosthetic knee and ankle/foot models as described in chapter IV. Due to the limitations of the current version of the simulation software, the prosthetic leg

segment lengths and mass properties were assumed to match those described in Winter's textbook (Winter, 2005) as listed in Appendix B. Earlier in chapter V & VI, the sound leg segment lengths and mass properties were assumed to be same as the prosthetic leg. In this chapter, the focus is on identifying the capability of the patient to approximate normal, rather than model simulation on the robot. This is the reason for the change. Furthermore, a prosthetic leg can be made heavier than its bare-bones structure, and some testing suggests that patients with a heavier prosthesis may have lower metabolic cost (Gaily et al., 1997, and Skinner & Mote, 1989). Inertial asymmetry between the sound and prosthetic leg may increase gait asymmetry (Bach , 1995, Mena at al., 1981, and Tsai & Mansour 1986).

7.2.2 Prosthetic knee model

The Mauch S-N-S modeled by this project is one of the most popular prosthetic knees on the market, and it includes separate adjustment functions for swing and stance damping. The representative dynamic model of the hydraulic cylinder of the Mauch Knee system was presented in chapter IV. We continue to use the simpler, more linear 2-phase model, which has so far proven adequate in simulations confirmed by testing.

With respect to damping setting options available during the flexion and extension phases of the Mauch knee, we selected the highest (F180E180), middle (F90E90), and lowest (F0E0) pairs for this study. The coefficients used in the mathematical models of the Mauch S-N-S are listed in table 7.

Table 7

Identified Parameters of 2-Phase Model

Damping setting	Coefficients	Low force section	High force section
F0E0	f_f (N)	-167.21	-241.99
	k (N/m)	12561.98	26295.64
	c (N•S/m)	872.37	16984.52
F90E90	f_f (N)	-189.91	-260.12
	k (N/m)	14115.95	28598.98
	c (N•S/m)	1415.05	17738.71
F180E180	f_f (N)	-213.85	-350.15
	k (N/m)	18745.24	59296.93
	c (N•S/m)	5318.22	23788.67

Note: F represents knee flexion and E represents knee extension. The number after F/E represents the level of damping resistance, the larger the number the higher of the damping resistance. That is, 0 is the lowest damping setting and 180 is the highest damping setting.

7.2.3 Prosthetic ankle/foot model

The question with respect to the prosthetic foot/ankle model in our system is "what should be the appropriate angular stiffness of the ankle joint in the simulation?" Hansen et al. (2004) have studied the moment-angle relationships of the ankle joint in able bodied subjects during gait. Based on their data, the torsional spring stiffness of the human ankle joint can be approximated as 450 Nm/rad. Lehmann et al. (1993) have studied the stiffness of three commercial prosthetic feet. From their study, the torsional spring stiffness of the Flex, Seattle, and SACH prosthetic feet can be approximated as 350, 600, and 700 Nm/rad. Based on this data, we selected the study values of stiffness shown by table 8.

Table 8

Range of studied prosthetic ankle/foot linear torsional spring stiffness

Stiffness (Nm/rad)	225	350	450	600	700	1000

The weight, height, and segment lengths of the hypothesized subject remain constant during all simulations. The only changes are the prosthetic knee damping and the foot/ankle stiffness. Three combinations of knee damping settings with a fixed 350 Nm/rad ankle stiffness (based on the Flex Foot performance) and six ankle/foot stiffnesses with fixed low damping setting (F0E0) were studied.

7.3 Results

Figure 23 compares the intact leg kinetics and kinematics of the hip, knee, ankle, and ground reaction forces (GRFs) of the hypothesized subject at slow walk at various damping settings with constant ankle stiffness. In each case this gait was determined to provide the optimal trade-off between gait kinematics and energy consumption, in accordance with the weights described in Chapter 5. Figure 24 provides the same comparisons for the prosthetic leg. Appendix C and D contain the comparisons of the intact and prosthetic leg kinetics and kinematics for normal and fast walk. Figure 25 compares the intact leg kinetics and kinematics with various torsional spring stiffness conditions and fixed, low damping. Figure 26 provides the prosthetic leg comparisons under these conditions. Note that the time axis for all the intact leg performance results are 50 % shifted compared to the prosthetic leg.

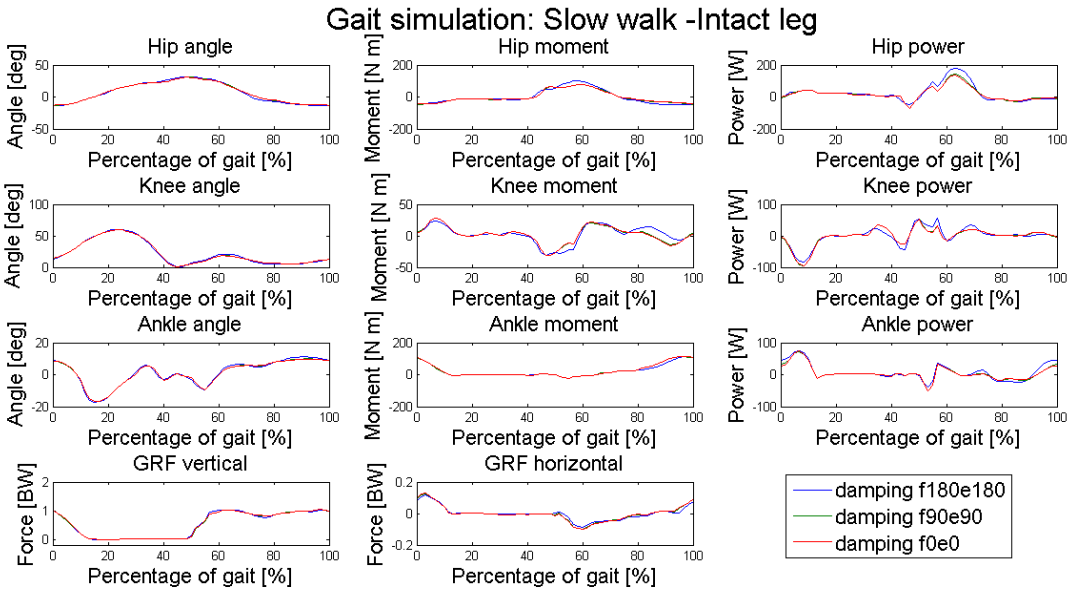

Figure 23: The intact leg kinetics and kinematics of the model subject wearing a Mauch knee system with various damping settings at slow walk. The torsional spring ankle stiffness of the simulations is 350 Nm/rad.

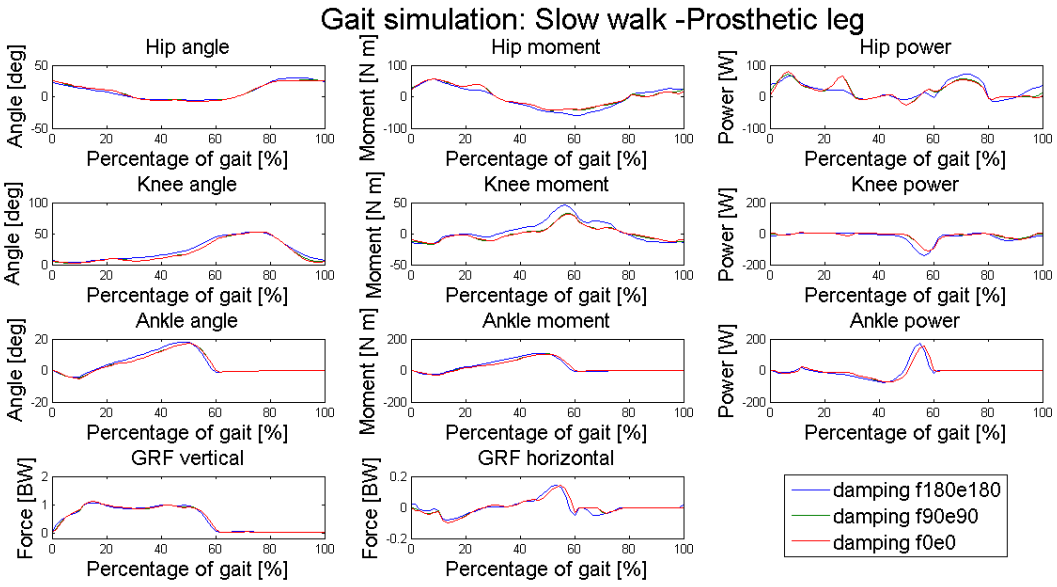

Figure 24: The prosthetic leg kinetics and kinematics of the model subject wearing a Mauch knee system with various damping settings at slow walk. The torsional spring ankle stiffness of the simulations is 350 Nm/rad

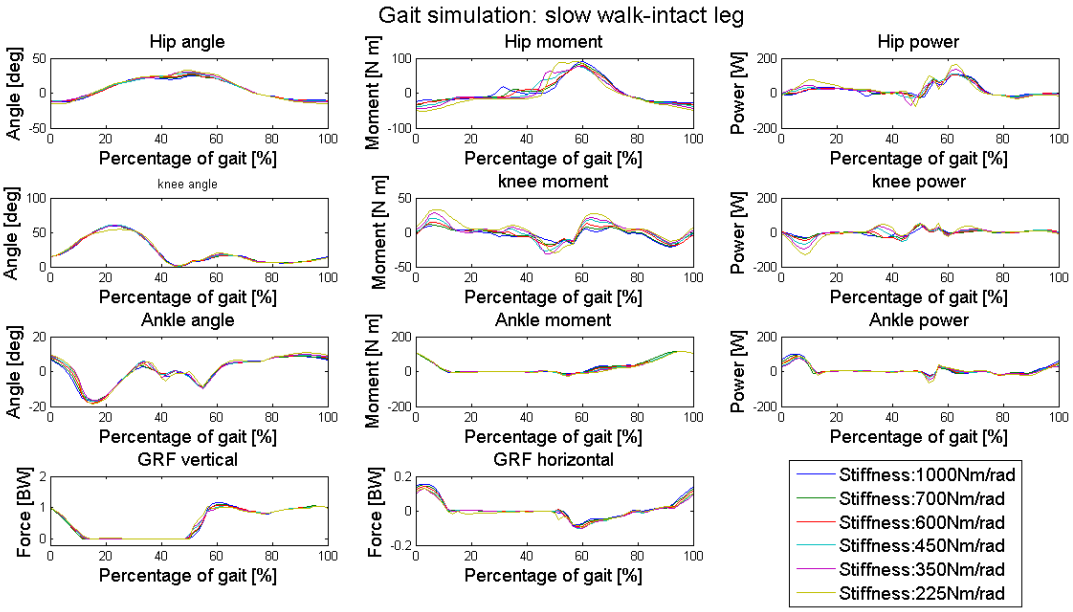

Figure 25: The intact leg kinetics and kinematics of the model subject wearing a Mauch knee system over a range of ankle stiffnesses. The damping resistance setting of the Mauch knee system is F0E0.

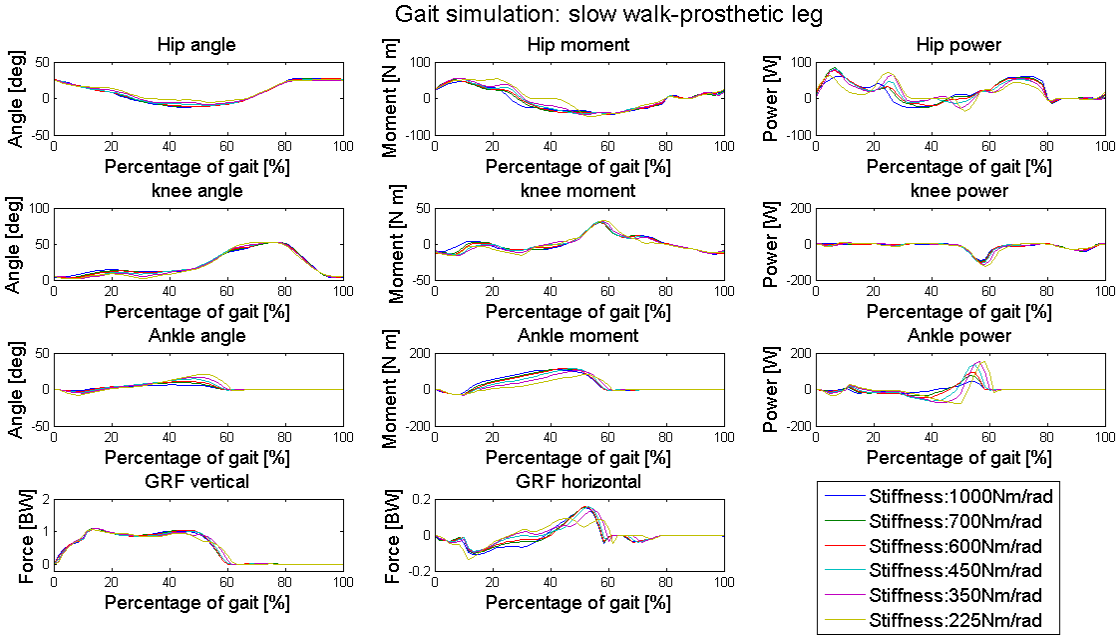

Figure 26: The prosthetic leg kinetics and kinematics of the model subject wearing a Mauch knee system over a range of ankle stiffnesses. The damping resistance setting of the Mauch knee system is F0E0.

7.4 Discussion

This study incorporates a number of assumptions and simplifications. The gait model is fundamentally two dimensional, and it is recognized that amputees may have

a significant amount of un-physiologic (and undesirable) out-of-plane motions and forces/moments. The model also requires a selection of weighting parameters for the relative priorities put on duplicating normal gait kinematics and on minimizing energy consumption. In a given clinical case these priorities might be different. A third issue with the software is that it currently requires the masses of both limbs to be identical. Prosthesis mass is known to effect gait kinematics and kinetics. With respect to the prosthetic leg model, some other choices also affect the result. Fundamentally, the prosthetic socket is idealized to have perfect behavior; no relative motions occur, forces and moments are transferred with 100% efficiency, and patient comfort is no issue. Study of socket issues is very important, but is not included in this study which has focused on the prosthetic knee and ankle. The simpler 2-phase model was chosen, over the 4-phase model we have also developed, to simplify and speed the analysis; as discussed in previous chapters this model appears to be adequate. Similarly, the ankle/foot is modeled as a simple torsional spring, to avoid the computational complexities of more involved models. The literature indicates that this is reasonable, and suggests that our data trends should be useful (Shamaei et al., 2011, & Lehmann et al., 1993).

Looking at the effects of knee damping and of ankle stiffness, a number of points become apparent. Figures 23 and 24 suggest that only small changes in the subject's gait kinetics and kinematics in either intact or prosthetic leg are observed over the range of damping resistance settings evaluated. In contrast, the simulations of various stiffnessess for the prosthetic ankle/foot show more significant effects on the kinetic and kinematic performance of the prosthetic and intact legs (Figure 25 & 26).

It is again noted that the simulated subject with Mauch knee system does not to activate the hyperextension mode after mid-stance phase, even though this feature of

the swing control is intended to reduce the resistance during swing phase. Apparently "optimal" gait, as defined for this study, does not require this design feature. The employment of this Mauch knee design feature is not reported on in the literature of amputee subject testing with this knee. Therefore, the realism of this aspect of the study is not easily evaluated.

Some data exists in the literature which can be compared to the simulation results. Segal et al. (2006) have studied the kinetics and kinematics of patients wearing Mauch SNS knees combined with a number of different commercial prosthetic feet. Their test subjects had an average height of 1.73±0.04 m and a weight of 79.6±10.4 kg; this is similar to our simulation subject who has height of 1.8 m and weight of 75 kg. Their controlled walking speed of 1.11±0.11 m/s was also similar to our simulation walking speed of 1.002 m/s. Table 9 & 10 provide the comparison of the kinetics and kinematics of the intact and prosthetic legs with Segal's data at various damping resistance settings at slow walk. Appendix E and F provide the comparison of the intact and prosthetic leg with Segal's data at various damping resistance settings at normal and fast walk. Table 11 & 12 provide the comparison of the kinetics and kinematics of the intact and prosthetic legs of the model subject with Segal's data at different foot/ankle stiffnesses.

Table 9

Kinetics and kinematics comparison of actual patients and simulation based on various damping setting of the Mauch S-N-S prosthetic knee at slow walk: Intact limb

	Segal's data	Simulation		
		Damping setting		
Biomechanical Variables		F0E0	F90E90	F180E180
Knee Kinematics (º)				
Peak Knee Flexion (early stance)	11.4±6	18.34	18.59	20.80
Knee Flexion (at opposite heel strike)	0.61±5	5.55	5.46	5.03
Peak Knee Flexion (swing)	52.9±4	59.86	59.82	60.57
Knee Kinematics (N•m/kg)				
Peak Knee Flexion Moment (early stance)	0.5±0.2	0.29	0.28	0.29
Hip Power (W/kg)				
H1 Power Maximum	0.72±0.6	1.80	1.90	2.41
H3 Power Maximum	0.67±0.1	0.59	0.60	0.54
Knee Power (W/kg)				
K1 Power Minimum	-0.74±0.4	-0.24	-0.23	-0.23
K3 Power Minimum	-0.38±0.2	-1.28	-1.29	-1.11
Ankle Power (W/kg)				
A2 Power Maximum	3.65±0.8	0.99	0.97	1.00
Vertical GRF				
Peak GRF from 10%-30% of gait cycle (% BW)	114±8	101.13	101.60	102.94
Time of Peak GRF (s)	0.156±0.04	0.18	0.18	0.18
		63.33	63.33	63.33
Hip Kinematics (º)				
Peak Hip Flexion		30.72	30.78	31.51
Peak Hip Extension		-12.78	-12.88	-13.96
Ankle Kinematics (º)				
Peak Ankle Flexion		9.75	9.90	11.23
PeakAnkle Extension		-16.63	-16.65	-17.14

Note. Walking Speed: 1.002 m/s; gait cycle: 1.383 sec per cycle.

Table 10

Kinetics and kinematics comparison of actual patients and simulation based on various damping setting of the Mauch S-N-S prosthetic knee at slow walk

	Segal's data	Simulation		
		Damping setting		
Biomechanical Variables		F0E0	F90E90	F180E180
Knee Kinematics (º)				
Peak Knee Flexion (early stance)	-4.3±5	9.39	9.36	10.68
Knee Flexion (at opposite heel strike)	-2.5±6	5.27	5.50	8.54
Peak Knee Flexion (swing)	64.4±6	52.46	52.39	51.89
Knee Kinematics (N•m/kg)		-1.79	-1.78	-0.98
Peak Knee Flexion Moment (early stance)	0.067±0.07	-0.02	-0.02	-0.01
Hip Power (W/kg)				
H1 Power Maximum	0.49±0.2	1.05	0.95	0.89
H3 Power Maximum	0.83±0.3	0.72	0.75	0.97
Knee Power (W/kg)				
K1 Power Minimum	N/A	-0.16	-0.15	-0.24
K3 Power Minimum	N/A	-1.49	-1.52	-1.94
Ankle Power (W/kg)				
A2 Power Maximum	N/A	2.05	2.07	2.29
Vertical GRF				
Peak GRF from 10%-30% of gait cycle (% BW)	100.3±7.5	110.39	110.31	106.35
Time of Peak GRF (s)	0.182±0.05	0.21	0.21	0.21
		15.00	15.00	13.33
Hip Kinematics (º)				
Peak Hip Flexion		25.33	26.20	30.33
Peak Hip Extension		-7.91	-7.64	-5.55
Ankle Kinematics (º)				
Peak Ankle Flexion		17.05	17.13	18.01
PeakAnkle Extension		-5.11	-5.05	-4.32

Note. Walking Speed: 1.002 m/s; gait cycle: 1.383 sec per cycle.

Table 11

Kinetics and kinematics comparison of actual patients and simulation based on various linear torsional spring stiffness of the prosthetic ankle at slow walk

Biomechanical Variables	Segal's data	Simulation Ankle Stiffness (N-m/rad)					
		225	350	450	600	700	1000
Knee Kinematics	(º)						
Peak Knee Flexion (early stance)	11.4±6	19.91	18.34	16.92	16.49	16.55	16.81
Knee Flexion (at opposite heel strike)	0.61±5	5.50	5.55	5.53	5.38	5.63	5.43
Peak Knee Flexion (swing)	52.9±4	54.19	59.86	60.98	60.50	59.80	59.58
Knee Kinematics (N•m/kg)							
Peak Knee Flexion Moment (early stance)	0.5±0.2	0.37	0.29	0.24	0.17	0.11	0.10
Hip Power (W/kg)							
H1 Power Maximum	0.72±0.6	2.17	1.80	1.48	1.38	1.43	1.43
H3 Power Maximum	0.67±0.1	0.99	0.59	0.43	0.39	0.39	0.47
Knee Power (W/kg)							
K1 Power Minimum	-0.74±0.4	-0.31	-0.24	-0.19	-0.13	-0.09	-0.07
K3 Power Minimum	-0.38±0.2	-1.70	-1.28	-0.94	-0.59	-0.46	-0.43
Ankle Power (W/kg)							
A2 Power Maximum	3.65±0.8	1.16	0.99	1.03	1.17	1.22	1.35
Vertical GRF							
Peak GRF from 10%-30% of gait cycle (% BW)	114±8	102.35	101.13	102.32	106.91	110.05	116.35
Time of Peak GRF (s)	0.156±0.04	0.07	0.13	0.12	0.12	0.12	0.10
Hip Kinematics (º)							
Peak Hip Flexion	N/A	32.48	30.72	28.95	26.85	26.40	24.97
Peak Hip Extension	N/A	-15.44	-12.78	-11.73	-10.94	-11.46	-12.08
Ankle Kinematics (º)							
Peak Ankle Flexion	N/A	9.75	9.75	9.48	9.39	8.77	8.70
PeakAnkle Extension	N/A	-16.63	-16.63	-17.16	-18.15	-16.52	-17.02

Note. Walking Speed: 1.002 m/s; gait cycle: 1.383 sec per cycle.

Table 12

Kinetics and kinematics comparison of actual patients and simulation based on various linear torsional spring stiffness of the prosthetic ankle at slow walk: Prosthetic limb

Biomechanical Variables	Segal's data	Simulation Ankle Stiffness (N-m/rad)					
		225	350	450	600	700	1000
Knee Kinematics	(º)						
Peak Knee Flexion (early stance)	-4.3±5	8.41	9.39	10.85	12.62	13.68	14.76
Knee Flexion (at opposite heel strike)	-2.5±6	2.31	5.27	8.19	10.44	10.95	11.38
Peak Knee Flexion (swing)	64.4±6	52.38	52.46	52.44	52.30	52.21	52.15
Knee Kinematics (N•m/kg)							
Peak Knee Flexion Moment (early stance)	0.067±0.07	-0.04	-0.02	0.00	0.01	0.03	0.05
Hip Power (W/kg)							
H1 Power Maximum	0.49±0.2	0.96	1.05	1.11	1.02	1.12	0.81
H3 Power Maximum	0.83±0.3	0.60	0.72	0.71	0.74	0.76	0.81
Knee Power (W/kg)							
K1 Power Minimum	N/A	-0.18	-0.16	-0.12	-0.07	-0.06	-0.08
K3 Power Minimum	N/A	-1.64	-1.49	-1.46	-1.38	-1.31	-1.26
Ankle Power (W/kg)							
A2 Power Maximum	N/A	2.02	2.05	1.84	1.28	1.01	0.61
Vertical GRF							
Peak GRF from 10%-30% of gait cycle (% BW)	100.3±7.5	108.06	110.39	109.63	109.16	110.13	110.12
Time of Peak GRF (s)	0.182±0.05	0.13	0.15	0.15	0.15	0.13	0.13
Hip Kinematics (º)							
Peak Hip Flexion	N/A	26.22	25.33	25.74	27.02	26.76	27.71
Peak Hip Extension	N/A	-5.14	-7.91	-9.23	-10.48	-11.01	-12.15
Ankle Kinematics (º)							
Peak Ankle Flexion	N/A	14.43	17.05	14.41	11.00	9.27	6.20
PeakAnkle Extension	N/A	-3.78	-5.11	-3.77	-2.74	-2.25	-1.52

Note. Walking Speed: 1.002 m/s; gait cycle: 1.383 sec per cycle.

Comparing the kinematics of the model simulation at various damping settings (Table 9) with Segal's data, the simulated intact leg has higher peak knee flexion during swing phase. However the knee motion during the stance phase (the angle difference between peak knee flexion and knee flexion at opposite heel strike) is similar to Segal's data. On the prosthetic leg side, the simulations have lower peak knee flexion during swing phase. The knee motion during the stance phase is similar to Segal's data. Kinematically, comparing the angle differences between the peak knee flexion angle during stance and swing phase for both intact and prosthetic leg, Segal's data has an average 41.5 degree difference for the intact leg and an average 68.7 degree difference for the prosthetic leg while the simulation results showed 39.77-41.32 degree difference for the intact leg and 41.21-43.07 degree difference for the prosthetic leg. Among the three damping settings, with respect to kinetic variables, the simulation results showed increased maximum H1 hip power for the intact and prosthetic legs and increased maximum K3 knee power for the simulated intact leg compared to Segal's data. It also showed maximum H3 hip power for the intact and prosthetic leg, lower K1 power for the prosthetic leg, and a significantly reduced maximum A2 ankle power for both legs. Furthermore, the results showed potentially reduced peak GRFs for the intact leg and more symmetric peak GRF between intact and prosthetic legs when the prosthetic knee is at the highest damping setting. The simulation results suggest that, although increased damping setting does not help to improve the kinetics or kinematics of gait but it may have the potential to make the gait more symmetrical with reduced peak or more symmetrical GRF. These issues have been indicated as causes of hip joint degeneration in amputees (Farahmand et al., 2006, & Gailey et al. 2008).

In the stiffness variation simulation results, the effect of ankle stiffness on gait performance is more significant than the effects of damping setting. Kinematically, the subject has the smallest peak flexion differences during stance and swing phase between intact (43.06 degree) and prosthetic (41.59 degree) legs with an ankle stiffness of 450 Nm/rad. This value approximates the natural ankle stiffness. The maximum peak flexion difference during stance and swing phase between intact (34.28 degree) and prosthetic (43.97 degree) leg occurred with an ankle stiffness of 225 Nm/rad. Kinetically, increasing the ankle stiffness may reduce the maximum H1, H3, K1, and K3 powers for both legs. Overall, the results showed the lowest peak joint powers at an ankle stiffness of 1000 Nm/rad. Furthermore, lowering ankle stiffness can also help to reduce the peak GRF for both intact and prosthetic legs.

7.5 Conclusion

This first use of simulation to evaluate the effect of specific prosthetic component parameters on gait performance was intended as a demonstration of the methodology, and not as the last word on the factors considered. While the analysis incorporated many approximations, the absence of socket dynamics and higher prosthetic mass among them, comparison to patient test data suggest that the results are reasonable. A patient/subject ambulating with the defined optimization goals may not effectively use the “stance and swing” feature of a Mauch knee; similarly, the damping may not have powerful effect on gait kinematic quality and power consumption. The ankle/foot stiffness is a powerful effect on the gait, with competing effects on the goals of kinematic and kinetic optimization. Proper choice of parameters may help make gait more symmetrical, with lower forces, which will be beneficial with respect to hip degeneration. From a gait quality point of view, if perhaps not patient stability and confidence, patients would appear to benefit from

careful system design of the ankle prosthesis more than from increasingly sophisticated knees. By comparing with Segal's test data, the results have also suggest that patients have the potential to improve their gait pattern without changing the prosthetic knee and ankle system.

CHAPTER VIII

SUMMARY AND CONCLUSION

8.1 Key Results from this study

The potential optimal gait pattern of patients wearing a prosthetic leg based on the Mauch S-N-S prosthetic knee and a linear torsion prosthetic foot/ankle has been studied through a sequential process of (1) Mauch knee mathematical model development, (2) integration of the Mauch knee model into the Gait2D simulation software, (3) validation of the Gait2D simulation result with a robotic gait simulator, (4) evaluation of the effect of the knee damping and foot/ankle stiffness to patient's gait, (5) comparison of the potential optimal gait pattern from simulation to gait pattern of actual patients wearing Mauch knee.

(1) Mauch knee mathematical model development: With appropriately adjusted gait patterns as test input data, we have successfully generated output data which show that designed functionalities of the Mauch knee have been exercised during the test. Later, the test output data were utilized to develop two types of Mauch knee model, the 2-phase model considers only the major characteristics of the test data and the 4-phase model which incorporates knowledge of the Mauch mechanism operation as well as the test data. The 2-phase model is a simpler, more linear model. The more complex 4-phase model predicts the component dynamics of the Mauch knee more accurately but the 2-phase model is more easily handled by the numerical solver algorithms when incorporated in a complex gait simulation. Results of the system simulation were good with the simple knee model. A finding was that under the assumptions of the study the hyperextension mode of the Mauch knee was not

activated; this is the performance region where the 4-phase model was most useful for improving component performance modeling.

(2) Integration of the Mauch knee model into the Gait2D simulation software: The available Gait2D musculoskeletal simulation program, the 2-phase knee model and a representative linear torsional spring model of the prosthetic foot/ankle were successfully integrated. During the simulation studies, a sequential process was used to acquire converged optimal solutions; (1) Healthy subject gait simulation: the average gait date from Winter's (2005) textbook were used as initial guess to simulate the optimal gait pattern of health subject, and the result was used as a starting point to simulate (2) a transtibial amputee's gait: where the ankle muscles on the right leg were removed and replaced by a linear torsion spring with a specified stiffness value. The result of transtibial simulation was used as the starting point to simulate (3) transfemoral amputee's gait: where the knee muscles of the right leg were removed and replaced by the Mauch knee model.

Our studies suggested that the Mauch knee is not a limiting factor in transfemoral amputee gait quality; under the assumptions made, the Mauch knee enabled much closer to normal gait than patients routinely achieve. As already noted, it was also found that the Mauch switching mechanism was not activated during optimal gait.

Generally, a single optimal solution was obtained in a reasonable amount of time, from 30 to 120 minutes, on an AMD Athlon™ X2 5400 desktop computer.

At present, Gait2D's formulation does impose some significant constraints on the model. These are:

(1) The prosthetic and intact legs must have the same mass distribution

(2) The residual hip muscles on the amputated side must have the same performance as on the non-surgical side.

(3) The importance of its two dimensional limitation can be debated. Normal gait has only a small component of out-of-plane- motion (Nielson & Daugaard, 2008), and ideally an amputee would be able to walk near normally with a prosthesis. At the same time, it is known that most amputees do not have a symmetrical gait pattern, which is a source of significant morbidities. It is a common observation of prosthetists that their clients walk much closer to a normal pattern when they are watched than they do when they think observation has ended. Simulations which have the potential to predict actual amputee gait must have three dimensional capability; these might help quantify the advantages amputees seem to find in abnormal gait.

For a complete system study, the ultimate prosthetic simulation model must include the socket-residual hip interface. Relative motions, poor alignment and pain in this area are major issues for patients. These may be very difficult to formulate mathematically. Testing of knees and ankles in a gait lab is probably significantly clouded by socket issues, and our approach has a major virtue in allowing developers of these components to remove the socket effects from the study.

(3) Validation of the Gait2D simulation result with robotic gait simulator: The first-generation robotic gait simulator proved very useful for testing a prosthetic leg under controlled conditions that included gait-like inputs. Closed loop control of the robot operation would extend the studies that could be performed, as would greater speed and load capability in its actuators. A method to vary ground stiffness may be useful, as might residual hip tissue axial and pelvic rotational stiffness simulations.

(4) Evaluation of the effect of the prosthetic knee damping and foot/ankle stiffness on patient's gait: 3 different prosthetic knee damping settings combined with specific foot/ankle stiffness and 6 different prosthetic foot/ankle stiffnesses combined with specified knee damping were simulated under assumed subject conditions. All combinations were run with slow, normal and fast walking speeds. The result showed that the foot/ankle stiffness has a more significant effect than the knee damping on the kinematics and kinetics performance of amputee gait. Damping of the prosthetic knee may still, however, provide some benefit with respect to gait symmetry.

(5) Comparison of the potential optimal gait pattern from simulation to the gait pattern of actual patients wearing Mauch knee: Segal's (2006) subjects were tested under conditions similar to the simulations, enabling comparisons. A list of the points of superior performance during our simulations is shown in table 13. The table indicates that our test subject under idealized condition has the potential to walk in a more symmetric manner with potentially reduced Maximum A2 power and more symmetric GRFs.

Table 13: *List of superior performance of simulation results with respect to Segal's data.*

	Segal's data	Damping	Ankle stiffness
(1) Gait kinematic symmetry (∘) (left and right leg differences)			
Peak Knee Flexion (early stance)	4.7 ~ 26.7	8.95 ~ 10.12	2.05 ~ 11.5
Knee Flexion (at opposite heel strike)	-7.89 ~ 14.11	-3.51 ~ 0.28	-5.95 ~ 3.19
Peak Knee Flexion (swing)	-21.5~ -1.5	7.4 ~ 8.68	1.8 ~ 8.54
(2) Significant Kinetics reduction			
Maximum A2 Power, (W/kg) (intact leg)	2.85 ~ 4.45	0.97~1.0	0.99 ~ 1.35

(3) Vertical GRF symmetry (left and right leg differences)			
Peak GRF from 10%-30% of gait cycle (% BW)	-1.8 ~ 29.2	-9.26 ~ -3.41	-9.26 ~ 6.23

Overall, we have successfully initiated the development of a methodology to evaluate the potential optimal performance of a prosthetic leg and its individual components. While significant additional development is required to fully represent all of the features of an amputee and a prosthetic leg, the ability to separate out the contributions of various factors to the net gait result has been clearly shown.

8.2 Future Studies

In summary, the methodologies developed here for creating prosthetic component models, incorporating them into musculoskeletal models, and performing system studies is highly practical and effective. Further development is warranted. The robotic testing has similar potential for testing prosthetic systems under controlled conditions.

The next critical research appears to be refinement of Gait2D, so that the mass distributions and muscle performance can differ between the intact and surgical sides. Some research may be necessary to determine the proper characterization of the residual muscles left by amputation.

More accurate foot/ankle models should be developed using techniques such as that used here for the knee, so that stiffness variations through the whole of stance can be incorporated; ankle stiffness is clearly a strong determinant of potential gait.

Socket models must be developed so that the impact of this component's performance on overall system behavior and the performance requirements for other components can be determined. It may also be useful to develop a prosthetic leg

model which will incorporate more details of its setup; prosthetists certainly spend significant time aligning the components to get the best patient results.

Ground stiffness must be evaluated and reported in computations or tests of prosthetic leg performance, if the forces and moments transmitted to the patient, the resulting energy consumptions, and the potential for related pathologies are to be fully understood. It may be that the stiffness of components now treated as rigid links such as the hip and pylon should be handled in a more sophisticated manner to obtain the best results for system studies.

Robotic testing, even with the first generation model used here, was very useful with respect to confirming the computations. Newer versions should be developed, with closed loop control and a greater range to the speed and force capabilities.

It appears clear that modern computational and test capabilities have the potential to reduce the need for human testing while speeding the development of improved prosthetic devices by providing more controlled and detailed evaluation of component performance and system interactions.

REFFERENCES

Ackermann M., van den Bogert A.J. (2010). Optimality principles for prediction of human gait. Journal of Biomechanics 43, 1055-1060.

Adalarasu, K., Jagannath, M., Mathur, M.K., (2011). Comparison on Jaipur, SACH and Madras Foot. International Journal of Advanced Engineered Sciences and Technologies. 4(1), 187-192.

Au, S. K., and Herr H. M.. (2008). Powered Ankle-Foot Prosthesis. Robotic and Automation Magazine. 52-59.

Bach, T.M.. (1995). Optimizing mass and mass distribution in lower limb prostheses. Prosthetics and Orthotics Australia. 29-35.

Bae, T. S., Choi, K., Hong, D., and Mu, M.. (2007). Dynamic Analysis of Above-Knee Aamputee Gait. Clinical Biomechanics 22, 557–566.

Bechtol, C. O., (1951). The Suction Socket. The Journal of American Medical Association. 146(7):625-628.

Beck, J.C., & Czerniecki, J.. (1994). A Method for Optimization of Above-Knee Prosthetic Shank-Foot Inertial Characteristics. Gait & Posture. 2, 75-84.

Blumentritt, S., Scherer, H.W., Michael, J.W. and Schmalz, T.. (1998). Transfemoral Amputees Walking on a Rotary Hydraulic Prosthetic Knee Mechanism: A Pre-Liminary Report, Journal of Prosthetics and Orthotics, 10(3), Pp 61-70.

Burke M. J., Roman V., and Wright V.. (1978). Bone and Joint Changes in Lower Limb Amputees. Annals of the Rheumatic Diseases, 37, 252-254.

Cappozzo, A., Leo, T., and Cortesi S. S.. (1980). A Polycentric Knee-Ankle Mechanism for Above-Knee Prostheses. Journal of Biomechanics. 13(3), 231-239.

Centers for Disease Control and Prevention. (2011). 2011 National Diabetes Fact Sheet. Retrieved from http://www.cdc.gov/diabetes/pubs/pdf/ndfs_2011.pdf.

Crowninshield, R.D., Brand, R.A. (1981). A physiological based criterion of muscle force prediction in locomotion. Journal of Biomechanical. 14(11), 793-801.

Dillingham, T. R., Pezzin, L. E., and Mackenzie, E. J.. (2002). Limb Amputation and Limb Deficiency: Epidemiology and Recent Trends in the United States. Southern Medical Journal, 95(8), 875-883.

Drills, R., Contini, R., and Bluestein, M.. (1964). Body Segment Parameters: A Survey of Measurement Techniques, 8(1), 44-66.

Edelstein, J. E.. (1998). Prosthetic Feet: State of the Art. Physical Therapy 68(12), 1875-1876.

Edwards, C., and Spurgeon, S.. (1998). Sliding mode control: Theory and application. Padstow: Taylor & Francis.

Ehde D. M., Smith D. G., Czerniecki J. M., Campbell K. M., Malchow D. M., Robinson L. R.. (2001). Back Pain as a Secondary Disability in Persons with Lower Limb Amputations. Archives of Physical Medicine and Rehabilitation. 82, 731-734.

Farahmand F., Rezaeian T., Narimani R. and Dinan P. H.. (2006). Kinematic and Dynamic Analysis of the Gait Cycle of Above-Knee Amputees. Scientia Iranica. 13(3), 261-271.

Faustini, M. C., Neptune, R. R., Crawford, R.H., Roger, W.E., and Bosker, G.. (2006). An Experimental and Theoretical Framework for Manufacturing Prosthetic Socket for Transtibial Amputees. Neural Systems and Rehabilitation Engineering, IEEE. 14(3), 304-310.

Ferris, D.P., Louise, M., and Farley, C.T.. (1998). Running in the real world: Adjusting leg stiffness for different surfaces. The Royal Society. 265, 989-994.

Gailey, R., Allen, K., Castles, J., Kucharik, J., & Roeder, M.. (2008). Review of Secondary Physical Conditions Associated with Lower Limb Amputation an Long-Term Prosthesis Use. Journal of Rehabilitation Research & Development. 45(1), 15-30.

Gaily, R.S., Nash, M.S., Atchley, T.A., Zilmer, R.M., Moline-Little, G.R., Morris, N., and Siebert, L.I.. (1997). The effects of prosthesis mass on metabolic cost of ambulation in non-vascular transtial amputees. Prosthetics and Orthotics International. 21, 9-16.

Gerritsen K. G. M., Nachbauer W., and van den Bogert A. J.. (1996). Computer Simulation of Llanding Movement in Downhill Skill: Anterior Cruciate Ligament Injuries. Journal of Biomechanics. 29(7), 845-854.

Giummarra, M. J., and Bradshaw, J. L.. (2010). The phantom of the night: Restless legs syndrome in amputees. Medical Hypotheses74, 968-972.

Godfrey, A., Conway, R., Meagher, D., and Ó Laighin, G.. (2008). Direct Measurement of Human Movement by Accelerometer. Medical Engineering & Physics. 30, 1364-1386.

Gogia, P. P., Braatz, J. H., Rose, S. J., and Norton, B. J.. (1987). Reliability and Validity of Goniometer Measurement at the Knee. Journal of the American Physical Therapy Association. 67, 192-195

Graham, L.E., Datta, D., Heller, B., Howitt, J.. (2007). A Comparative Study of Conventional and Energy-Storing Prosthetic Feet in High-Functioning Transfemoral Amputees. Archieve Physics Medicine Rehabilitation. l 88(6), 801-806.

Gudmundsson, K. H., Jonsdottir, F., and Thorsteinsson, F.. (2010). A Geometrical Optimization of a Magneto-Rheological Rotary Brake in a Prosthetic Knee. Smart Materials and Structures. 19.

Hobson, D.A., and Torfason, L.E.. (1975). Computational optimization of polycentric prosthetic knee mechanisms. Bulletin of Prosthetic Research. 187-201.

Hof, A. L., van Bockel, R. M., Schoppen, T., Postema, K.. (2007). Control of Lateral Balance in Walking Experimental Findings in Normal Subjects and Above-knee Amputees. Gait&Posture. 25, 250-258.

Horn, B. and Schunck, B., "Determining optical flow.," Artificial Intelligence,

Hoy, M.G., Zajac, F.E., and Gordon, M.E.. (1990). A Musculoskeletal model of the human lower extremity: The effect of muscle, tendon, and moment arm on the

moment-angle relationship of musculotendon actuators at the hip, knee, and ankle. Journal of Biomechanics. 23(2), 157-169.

Jaegers, S.M., Arendzen, J.H., de Jongh, H.J..(1995). Prosthetic Gait of Unilateral Transfemoral Amputees: A Kinematic Study. Archives of Physical Medicine and Rehabilitation. 76(8), 736-743.

KulKarni, J. (2008). Letter to editor:post amputation syndrome. Prosthetics and Orthotics International, *32*(4), 434-437.

Legro, M.W., Reiber, G., del Aguila, M., Ajax, M.J., Boone, D.A., Larsen, J.A., Smith, D.G., & Sangeorzan, B.. (1999). Issues of Importance Reported by Persons with Lower Limb Amputations Prostheses. Journal of Rehabilitation Research & Development. 36(3).

Lehmann J.F., Price R., Boswell-Bessette S., Dralle A., Questad K., and deLateur B.J.. (1993). Comprehensive analysis of energy storing prosthetic feet: Flex-Foot and Seattle Foot versusstandard SACH Foot. Archives of Physical Medicine and Rehabilitation. 74(11), 1225–31.

Ljung, L. (1999). System identification. (2nd ed.). Upper Saddle River: Prentice-Hall, Inc.

Mak, A. F.T., Zhang, M., and, Boone, D. A. (2001). State-of-the-art in lower-limb prosthetic biomechanics-socket interface: A review. Journal of Rehabilitation Research and Development. 38(2), 161-174.

Martin C. W.. (2003). Otto Bock C-leg® :A review of its effectiveness. WCB Evidence Based Group. 27.

Mauch H. A.. U.S. Patent 2,859,451, Hydraulic System, Nov. 11, 1958.

Mauch, H. A.. (1968). Stance control for above-knee artificial legs design considerations in the S-N-S knee. Bulletin of prosthetics research. Fall.

Mena, D., Mansour, J.M., and Simon, S.R.. (1981). Analysis and synthesis of human swing leg motion during gait and its clinical application. Journal of Biomechanics. 14(2), 823-832.

Michael J. (1987). Energy Storing Feet: A Clinical Comparison. Clinical Prosthetics and Orthotics 11(3), 154-68.

Mitchell, M., Craig, K., Kyberd, P., Biden, E., and Bush, G.. (2013). Design and Development of Ankle-Foot Prosthesis with Delayed Release of Plantarflexion. Journal of Rehabilitation Research & Development. 50(3), 409-422.

Nasseri, N, Hadian, M. R., Bagheri, H., Talebian, S., and Olyaei, G.. (2007). Reliability and Accuracy of Joint Position Sense Measurement in the Laboratory and Clinic; Utilizing a New System. Acta Media Iranica. 45(5), 395-404.

Nielson, D.B., and Daugaard, M.. (2008). Comparison of angular measurements by 2D and 3D gait analysis. School of health sciences, Jönköping University.

Norton, K. M.. (2007). A Brief History of Prosthetics. inMotion. 17(7).

Orendurff, M. S., Segal, A. D., Klute, G. K., McDowell, M. L., Pecoraro, J. A., and Czerniecki, J. M.. (2006). Gait efficiency using the C-Leg. Journal of Rehabilitation Research & Development. 43(2), 239-246.

Pai, D.K.. (2010). Muscle mass in musculoskeletal models. Journal of Biomechanics 43, 2093-2098.

Palmer, M.. (2002). Sagittal Plane Characterization of Normal Human Ankle Function Across a Range of Walking Gait Speeds. MS Thesis, Massachusetts Institute of Technology, Cambridge.

Perry, J., and Burnfield, J.M.. (2010). Gait Analysis: Normal and pathological function. Thorofare, NJ: Slack Inc.

Pfeifer, S., Reiner, R., and Vallery, H.. (2012). An Actuated Transfermoral Prosthesis With Optimized Polycentric Knee Joint. 4th IEEE RAS & EMBS International Conference on Biomedical Robotics and Biomechatronics.

Piazza, S.J., and Delp, S.L.. (1996). The Influence of Muscles on Knee Flexion During the Swing Phase of Gait. Journal of Biomechanics 29(6), 723-733.

Prince, F., Winter, D.A., Sjonnensen, G., Powell, C., & Wheeldon, R.K.. (1998). Mechanical Efficiency During Gait of Adult with transtibial Amputation: A Pilot Study Comparing the SACH, Seattle, and Golden-Ankle Prosthetic Feet.

Pritham, C. H.. Hydraulic/Pneumatic Knee Control Units: A Prosthetist's Point of View. Clinical Prosthetics and Orthotics: C.P.O. 7(4), 7-8.

Pritham, C.H.. (1983). Hydraulic/Pneumatic knee control units: A prosthetist's point of view. Clinical Prosthetics & Orthotics. 7(4), 7-8.

Prosthetic Socket Ambulation: Comparison of Finite Element Results with Experimental Measurements. Journal of Rehabilitation Research. 30(2), 191-204.

Richter, H., Simon, D., Smith, W. and Samorezov, S.. 2012. Development of a Leg Prosthesis Test Robot: Controls-Oriented Modeling and Parameter Estimation. ASME Journal of Biomechanical Engineering.

Rose, J., and Gamble, J. G.. (1994). Human Walking, Illustrated Ed.. Baltimore, MA: Williams & Wilkins.

Rosenbrock, H. H.. (1962/1963). Some general implicit processes for the numerical solution of differential equations. Computer Journal. 5, 329-330.

Sanders, J. E., and Daly, C. H.. (1993). Normal Shear Stresses on a Residual Limb in a Prosthetic Socket During Amputation: Comparison of Finite Element Results With Experimental Measurements. Journal of Rehabilitation Research & Development. 30(2), 191-204.

Sanderson, D.J., Martin, P.E.. (1997). Lower Extremity Kinematic and Kinetic Adaptations in Unilateral Below-Knee Amputees During Walking. Gait and Posture. 6, 126-136.

Saunders, J. B., M., Inman, V. T., and Eberhart, H. D.. (1953). The major determinants in normal and pathological gait. The journal of bone & joint surgery. 35, 543-558.

Schaffer E., Kort C., and Kreuter P., (2008). The prosthetic knee: microprocessor and non-microprocessor knee joints. *Inmotion.* 18(7), 34-36.

Schmalz, T., Blumentritt, S., Jarasch, R.. (2002). Energy expenditure and biomechanical characteristics of lower limb amputee gait: The influence of

prosthetic alignment and different prosthetic components. Gait and Posture 16, 255-263.

Segal A. D., Orendurff M. S., Klute G. K., McDowell M. L., Pecoraro J. A., Shofer J., Czerniecki J. M. (2006). Kinematic and kinetic comparisons of transfemoral amputee gait using C-Leg® and Mauch SNS® prosthetic knees. Journal of Rehabilitation Research & Development. 43(7), 857-870.

Seith, P.K.. (1972). A Rubber Foot for Amputees in Underdeveloped Countries. Journal of Bone and Joint Surgery. 54(B), 177-178.

Seth, A., Sherman, M., Reinbolt, J.A., and Delp, S.L.. (2011). Opensim: a musculoskeletal modeling and simulation framework for *in silico* investigations and exchange. Procedia IUTAM. 2(1), 186-198.

Shamaei, K., Cenciarini, M., & Dollar, A.M.. (2011, August 30th- September 3rd). On the Mechanics of the Ankle in the Stance Phase of the Gait. 33rd Annual International Conference of the IEEE EMBS. Boston, Massachusetts USA, (PP 8135-8140).

Singer, E., Ishai, G., and Kimmel, E.. (1995). Parameter estimation for a prosthetic leg. Annals of Biomedical Engineering. 23(5), 691-696.

Skinner HB, & Barrack RL. (1990). Ankle Weighting Effect on Gait in Able-Bodied Adults. Archives of Physical Medicine and Rehabilitation. 71, 112-115.

Skinner, H.B., and Mote, C.D.. (1989). Optimization of amputee prosthesis weight and weight distribution. Rehabilitation Research and Development Progress Report. 26, 32-33.

Smith D. G.. (2004). The transfemoral amputation level, part 1: Doc, it's 10 times more difficult!. inMotion. 14(2).

Strac, M., and Popovic, D. B.. (2012). Software Tool for Prosthetic Foot Modeling and Stiffness Optimization. Computational and Mathematical Methods in Medicine. 2012.

Strbac, M., and Popovic, D. B.. (2012). Software Tools for the Prosthetic foot Modeling and Stiffness Optimization. Computational and Mathematical Methods in Medicine. 2012.

Thelen, D. G., & Anderson, F. C.. (2006). Using computed muscle control to generate forward dynamic simulations of human walking from experimental data. Journal of Biomechanics 39, 1107–1115.

Tsai, C.S., and Mansour, J.M.. (1986). Swing phase simulation and design of above knee prostheses. Journal of Biomechanical Engineer. 108(1), 65-72.

Utkin, V.. (1992). Sliding modes in control optimization. Berlin: Springer-Verlag.

van den Bogert A.J., Davis B.L., Samorezov S., Smith W.. (2012) Modeling and Optimal Control of an Energy-Storing Prosthetic Knee. ASME Journal of Biomechanical Engineering. 134(5).

van den Bogert AJ, Blana D, Heinrich D (2011) Implicit methods for efficient musculoskeletal simulation and optimal control. Procedia IUTAM 2, 297-316. Open access at: http://www.sciencedirect.com/science/article/pii/S2210983811000289

Vanderwerker E. E. (1976). A Brief Review of the History of Amputations and Prostheses. Inter-Clinic Information Bulletin 15(5), 15-16

vol. 17, no. 1-3, pp. 185--203, 1981.

Wentink E. C., Rietman J. S., Veltink P.H., (2009). The feasibility of reflexive control in transfemoral prostheses. IEEE-EMBS Benelux Chapter Symposium.

Whittle, M. W.. (2007). An Introduction to Gait Analysis, 4th Ed.. Woburn, MA.: Butterworth-Heinemann.

Whittle, M.W.. (1996). Gait analysis: An introduction. (2nd ed.). Oxford: Butterworth-Heinemann.

Wiest, J., 2002. What's new in prosthetic knees? inMotion. 12(3), 36-40.

Williams, R. MTurner, A. P., Orendurff, M., Segal, A. D., Klute, G. K., Pecoraro, J., Czerniecki, J.. (2006). Does Having a Computerized Prosthetic Knee Influence Cognitive Performance During Amputee Walking?. Archives of Physical Medicine and Rehabilitation. 87, 989-994.

Wilson, A.B.. (1963). Limb prosthetics today. Artificial Limbs. 7(2), 1-42.wilson

Winter, D. A.. (2005). Biomechanics and motor control of human. (3rd ed.). Waterloo: John Wiley & Sons, INC.

Winer, D. A.. (1983). Energy generation and absorption at the ankle and knee during fast, natural, and slow cadences. Clinical Orthopaedics and Related Research. 23(6), 769-778.

Yokogushi, K., Narita, H., Uchiyama, E., Chiba, S., Nosaka, T., and Yamakoshi, K.. (2004). Biomechanical and Clinical Evaluation of a Newly Designed Polycentric Knee of Transfemoral Prosthesis. Journal of Rehabilitation Research & Development. 41(5), 675-682.

Martinez-Villalpando, E. C., & Herr, H.. (2009). Agonist-Antagonist Active Knee Prosthesis: A Preliminary Study in Level-Ground Walking. Journal of Rehabilitation Research & Development. 46(3), 361-374.

Fey, N. P., Klute, G. K., and Neptune, R. R.. (2013). Altering Prosthetic Foot Stiffness Influences Foot and Muscle Function During Below-Knee Amputee Walking: A modeling and Simulation Analysis. Journal of Biomechanics. 46(4), 637-644.

APPENDICES

APPENDIX A

Comparisons of Measured and Estimated System with 2-Phase Model and 4-Phase Model with Varios Cadences and Damping Settings

Dial Setting: F0E0

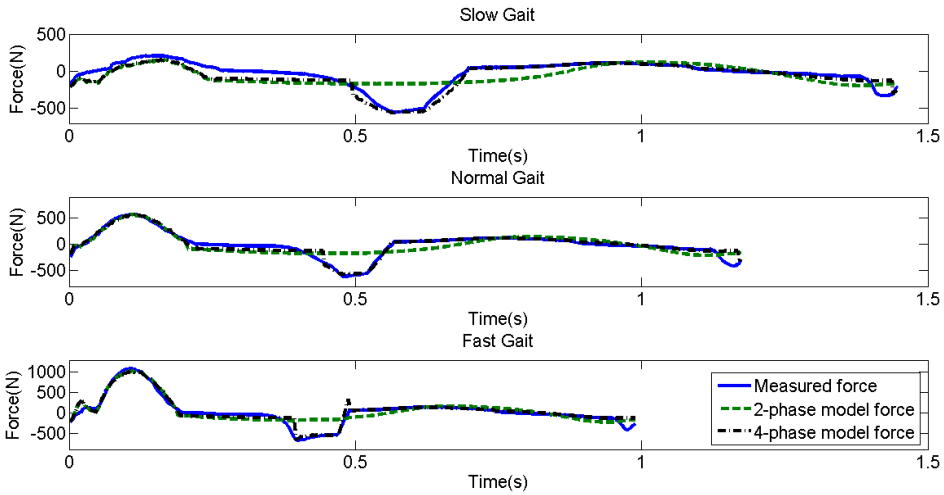

Dial Setting: F0E90

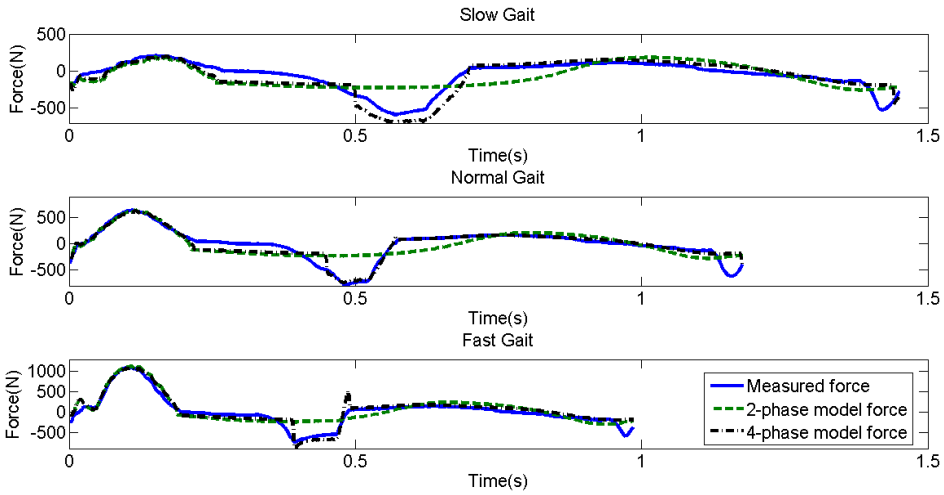

Dial Setting: F0E180

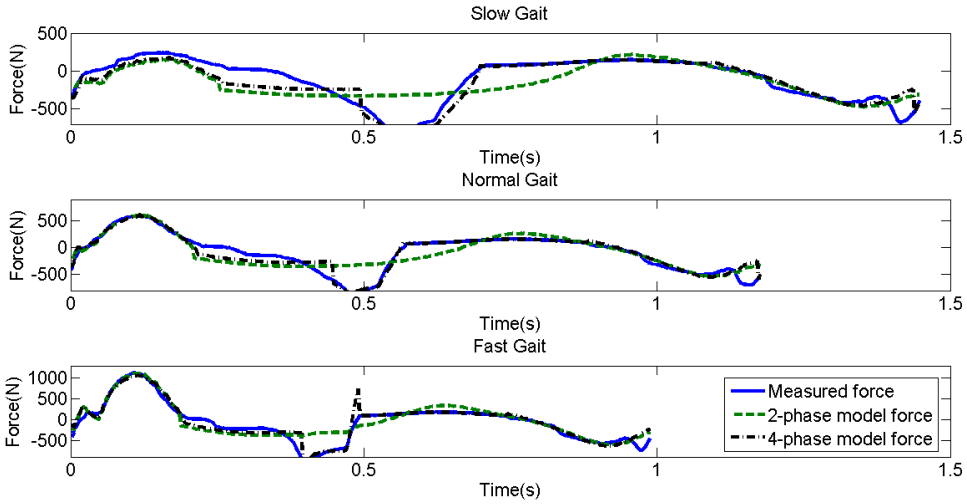

Dial Setting: F90E0

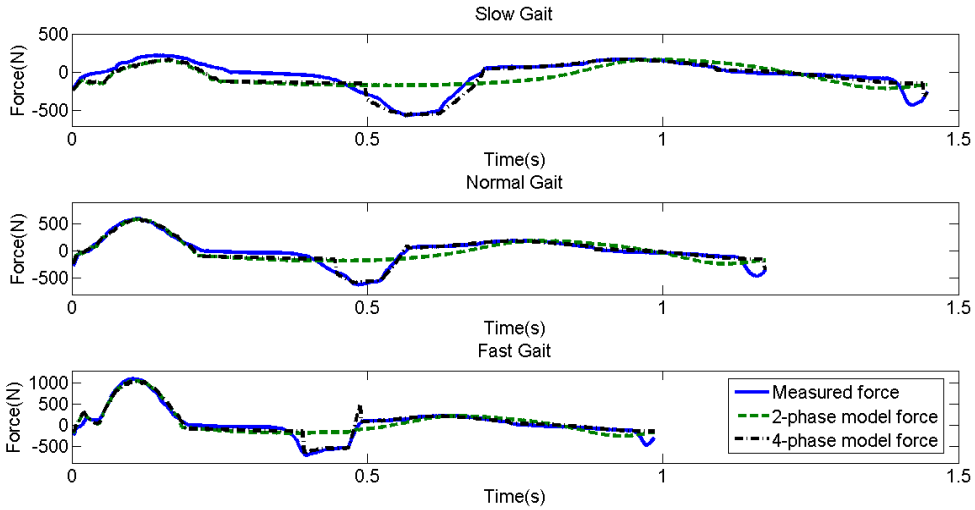

Dial Setting: F90E90

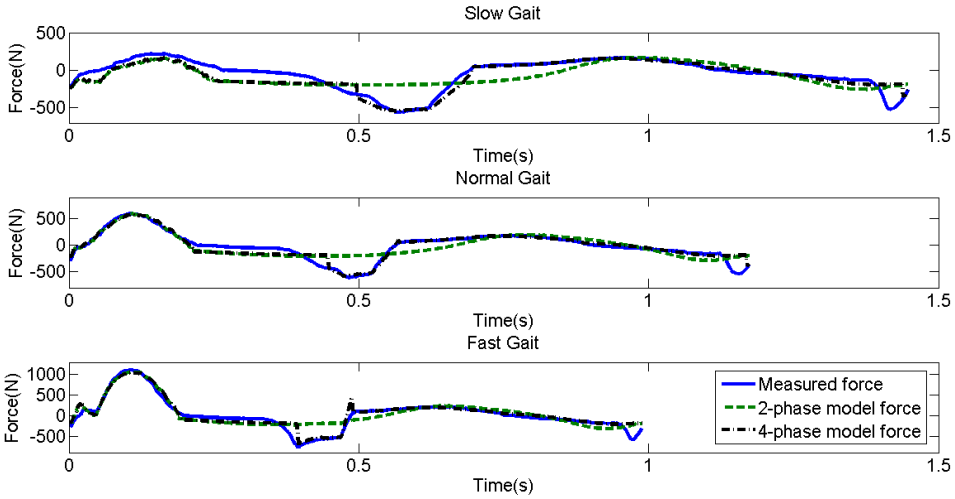

Dial Setting: F90E180

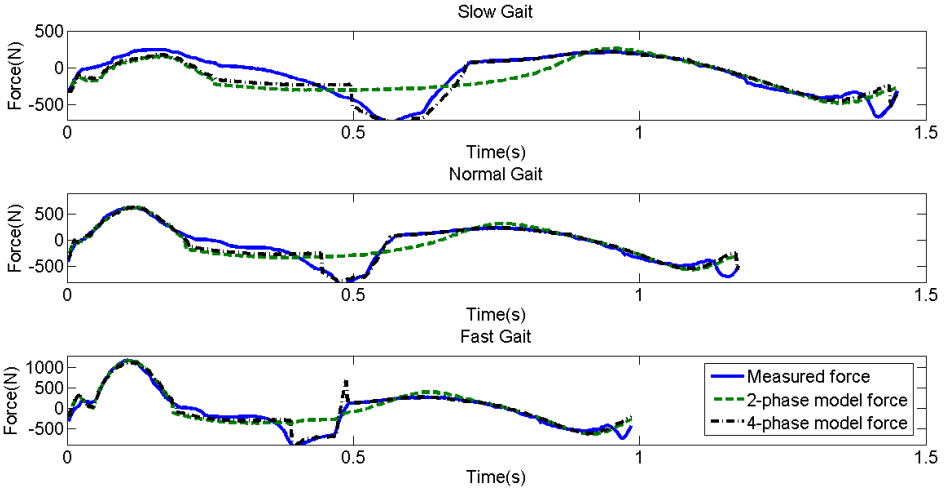

Dial Setting: F180E0

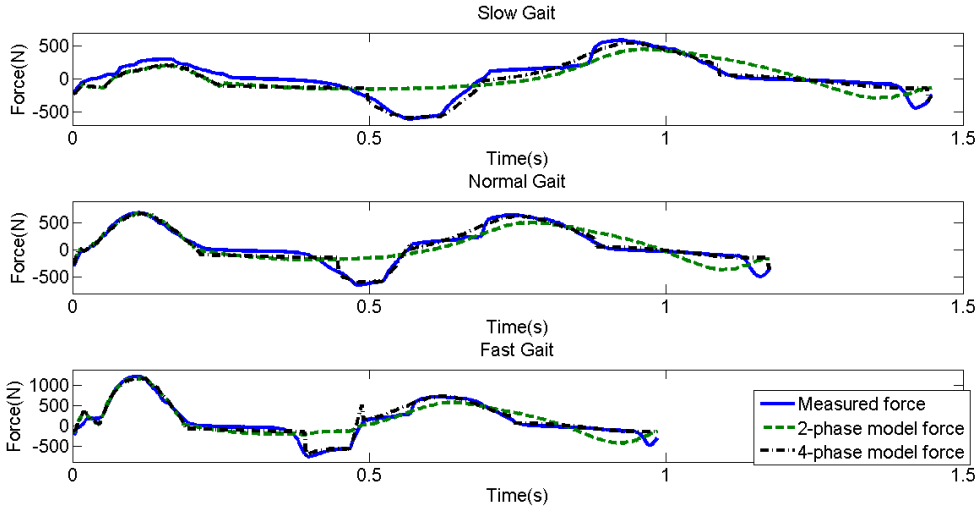

Dial Setting: F180E90

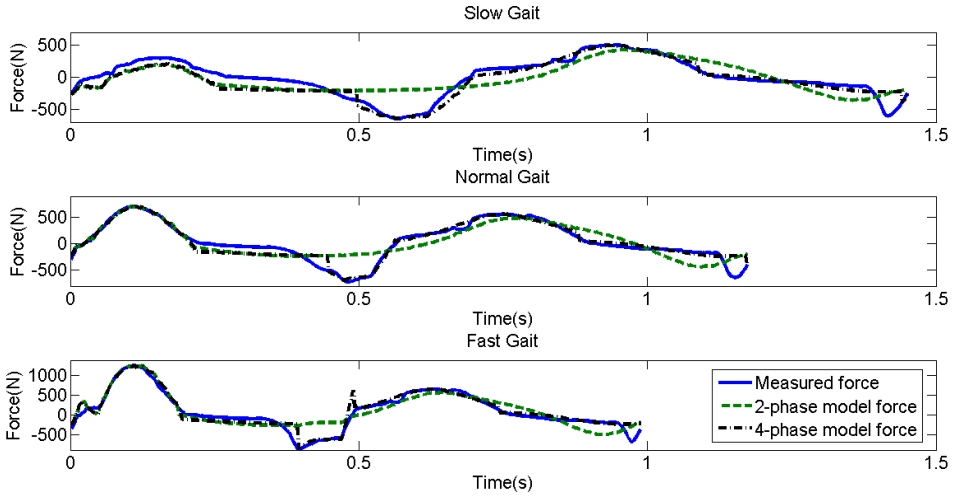

Dial Setting F180E180

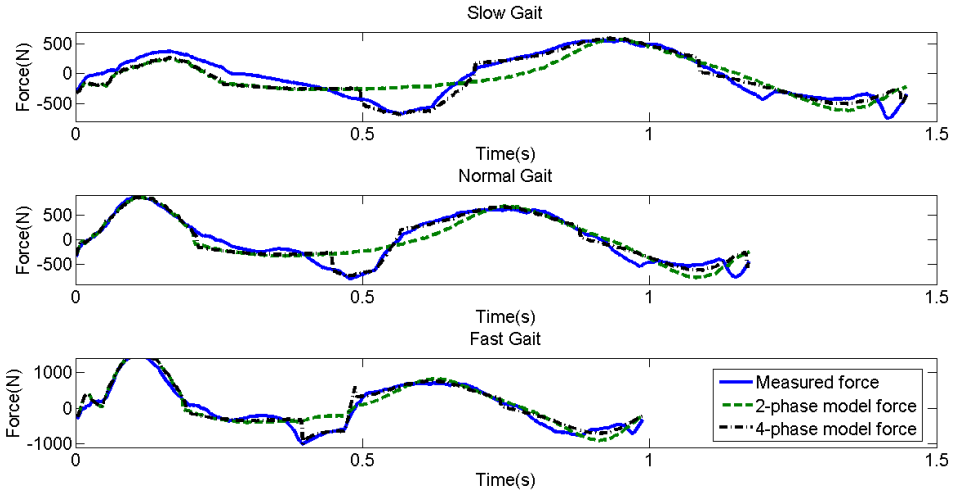

APPENDIX B

1 GENERAL PARAMETERS		
Stiffness	2.00E+04 [N/m]	Stiffness of ground contact (nominal value 1e5 N/m)
Damping	1.000 [s/m]	Damping parameter for ground contact force
ContactY0	0.00100 [m]	Deformation transition parameter in normal force model
ContactFric	1.000	friction coefficient
ContactV0	0.100 [m/s]	Transition speed for friction model
HillA	0.250	Normalized Hill constant "a" for muscles
Gmax	1.500	Maximal eccentric muscle force (normalized to Fmax)
Height	1.800 [m]	Body height
Mass	75.000 [kg]	Body mass

2 BODY SEGMENT PARAMETERS (Height and Mass using Winter, 2005)							
	Mass	Inertia	CMx	CMy	Length	Ankle Height	Heel-Ankle Disatance
HAT	50.8500	3.1777	0	0.3155	0.5040		
Thigh	7.5000	0.1522	0	-0.1910	0.4410		
Shank	3.4875	0.0624	0	-0.1917	0.4428		
Foot	1.0875	0.0184	0.0768	-0.0351	0.2736	0.0702	0.06

3 MUSCLE PARAMETERS								
Right	Iliopsoas	Glutei	Hamstrings	Rectus	Vasti	Gastroc	Soleus	TibialisAnt
Fmax	1500	3000	3000	1200	7000	3000	4000	2500
Lceopt	0.102	0.2	0.104	0.081	0.093	0.055	0.055	0.082
Width	1.298	0.625	1.197	1.443	0.627	0.888	1.039	0.442
PEEslack	1.2	1.2	1.2	1.4	1.4	1.2	1.2	1.2
SEEslack	0.142	0.157	0.334	0.398	0.223	0.42	0.245	0.317
kPEE	1	1	1	1	1	1	1	1
umax	0.05	0.05	0.05	0.05	0.05	0.05	0.05	0.05
Vmax	10	10	10	10	10	10	10	10
Tact	0.05	0.05	0.05	0.05	0.05	0.05	0.05	0.05
Tdeact	0.06	0.06	0.06	0.06	0.06	0.06	0.06	0.06
L0	0.248	0.271	0.383	0.474	0.271	0.487	0.284	0.381
dRhip	0.05	-0.062	-0.072	0.034	0	0	0	0
dRknee	0	0	-0.034	0.05	0.042	-0.02	0	0
dRankle	0	0	0	0	0	-0.053	-0.053	0.037
dLhip	0	0	0	0	0	0	0	0
dLknee	0	0	0	0	0	0	0	0
dLankle	0	0	0	0	0	0	0	0
Left	Iliopsoas	Glutei	Hamstrings	Rectus	Vasti	Gastroc	Soleus	TibialisAnt
Fmax	1500	3000	3000	1200	7000	3000	4000	2500
Lceopt	0.102	0.2	0.104	0.081	0.093	0.055	0.055	0.082
Width	1.298	0.625	1.197	1.443	0.627	0.888	1.039	0.442
PEEslack	1.2	1.2	1.2	1.4	1.4	1.2	1.2	1.2
SEEslack	0.142	0.157	0.334	0.398	0.223	0.42	0.245	0.317

kPEE	1	1	1	1	1	1	1	1
umax	0.05	0.05	0.05	0.05	0.05	0.05	0.05	0.05
Vmax	10	10	10	10	10	10	10	10
Tact	0.05	0.05	0.05	0.05	0.05	0.05	0.05	0.05
Tdeact	0.06	0.06	0.06	0.06	0.06	0.06	0.06	0.06
L0	0.248	0.271	0.383	0.474	0.271	0.487	0.284	0.381
dRhip	0	0	0	0	0	0	0	0
dRknee	0	0	0	0	0	0	0	0
dRankle	0	0	0	0	0	0	0	0
dLhip	0.05	-0.062	-0.072	0.034	0	0	0	0
dLknee	0	0	-0.034	0.05	0.042	-0.02	0	0
dLankle	0	0	0	0	0	-0.053	-0.053	0.037

Definitions of muscle parameters

Fmax	[N]	Maximal isometric muscle force
Lceopt	[m]	Length at which contractile element (CE) can produce its highest force
Width		Half width of the CE force-length relationship, relative to Lceopt
PEEslack		Slack length of the parallel elastic element (PEE), relative to Lceopt
SEEslack	[m]	Slack length of the series elastic element (SEE), in meters
kPEE		Stiffness parameter of PEE, normalized to Fmax and Lceopt
umax		Strain in SEE when loaded by Fmax of muscle
Vmax	[s^-1]	Maximum shortening velocity, normalised to Lceopt
Tact,Tdeact	[s]	Activation and deactivation time constants of muscle
L0	[m]	Muscle+tendon length when all joint angles are zero
dXXX	[m]	Moment arm of muscle with respect to joint XXX. Positive when muscle causes anterior swing of distal segment.

APPENDIX C

Simulation results of normal walking kinetics and kinematics of the model subject wearing a Mauch knee system with respect to a range of Mauch knee damping settings. The torsional spring ankle stiffness of the p simulation is 350 Nm/rad.

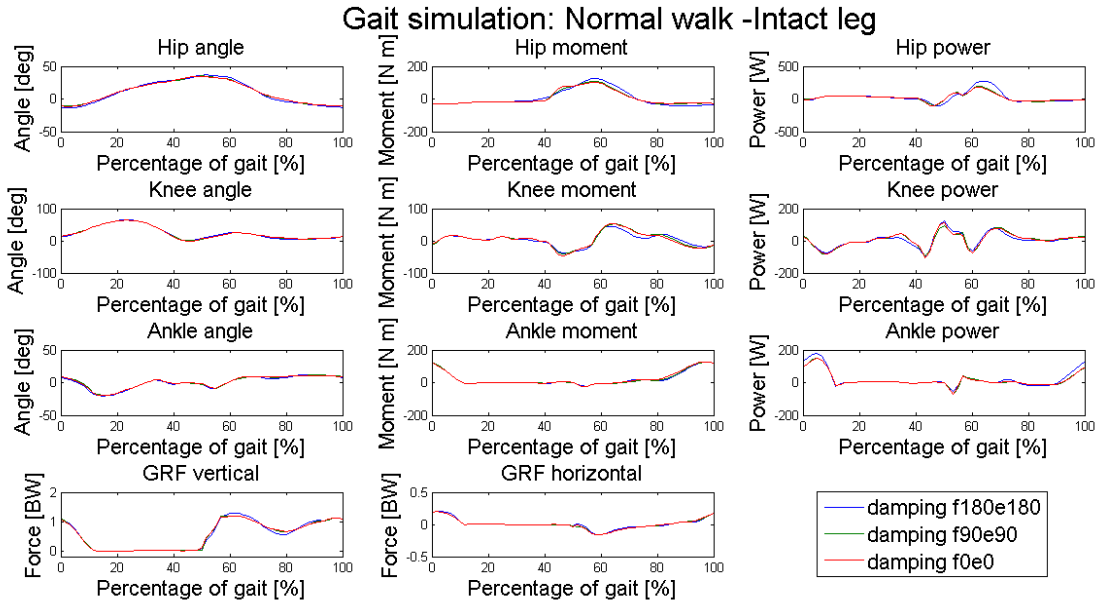

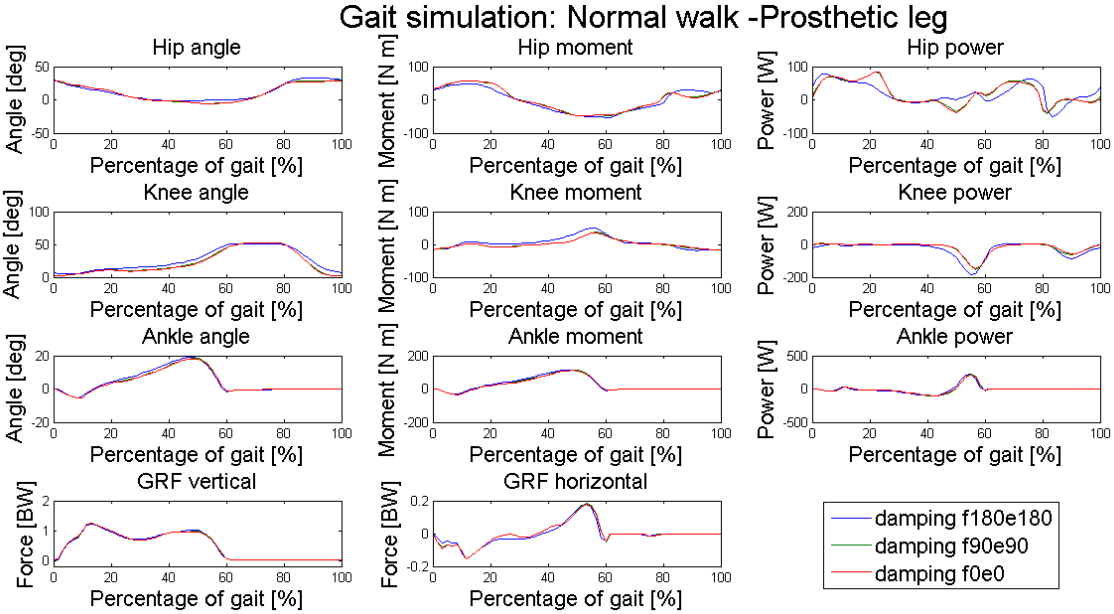

APPENDIX D

Simulation results of fast walking kinetics and kinematics of the model subject wearing a Mauch knee system with respect to a range of Mauch knee damping settings. The torsional spring ankle stiffness of the p simulation is 350 Nm/rad.

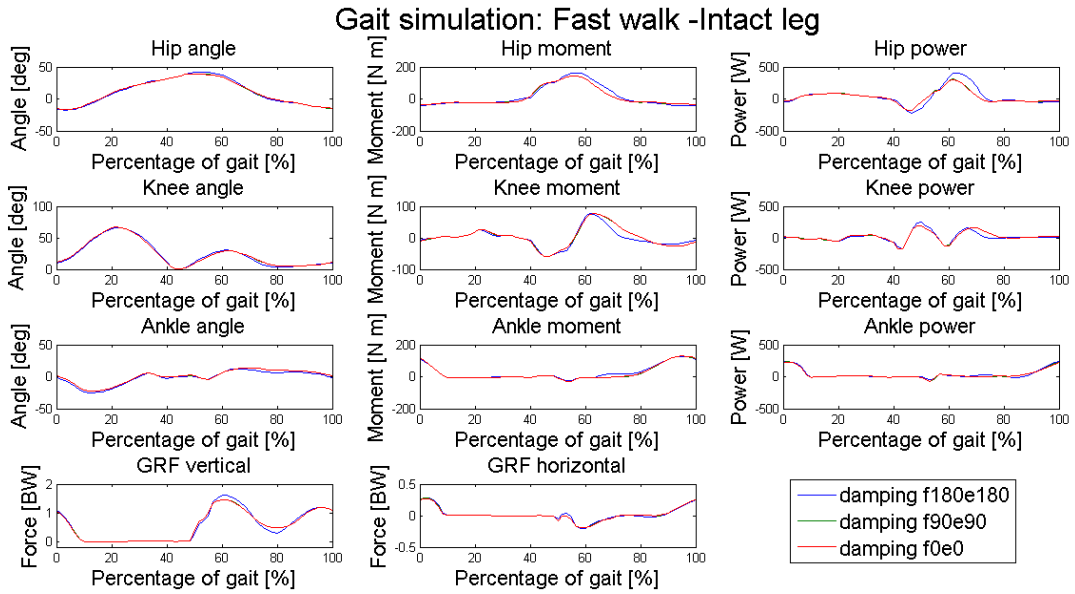

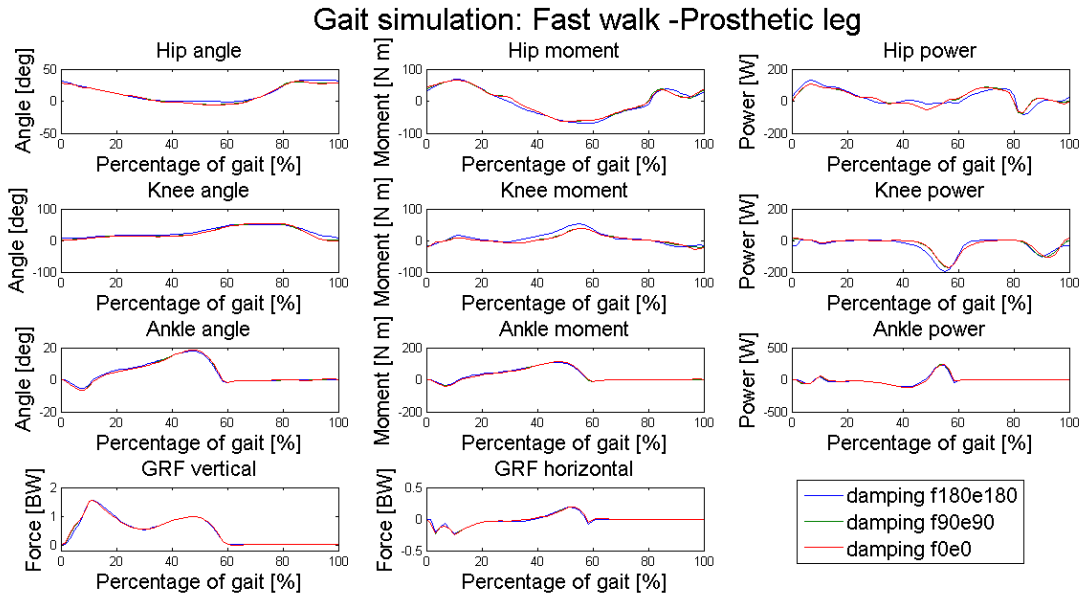

APPENDIX E

Kinetics and kinematics comparison of actual patients and simulation based on varios damping setting of the Mauch S-N-S prosthetic knee at normal walking

Intact Limb			
Biomechanical Variables	F0E0	F90E90	F180E180
Knee Kinematics (º)			
Peak Knee Flexion (early stance)	24.6135	24.58	25.40
Knee Flexion (at opposite heel strike)	5.90	5.37	4.97
Peak Knee Flexion (swing)	63.82	63.88	65.53
Knee Kinematics (N•m/kg)			44.95
Peak Knee Flexion Moment (early stance)	0.70	0.69	0.60
Hip Power (W/kg)			
H1 Power Maximum	2.37	2.56	3.66
H3 Power Maximum	0.68	0.67	0.69
Knee Power (W/kg)			
K1 Power Minimum	-1.01	-1.01	-0.81
K3 Power Minimum	-1.06	-1.10	-1.00
Ankle Power (W/kg)			
A2 Power Maximum	1.96	1.99	2.36
Vertical GRF			
Peak GRF from 10%-30% of gait cycle (% BW)	118.92	119.95	129.30
Time of Peak GRF (s)	0.13	0.13	0.13
Hip Kinematics (º)			
Peak Hip Flexion	35.00	35.20	38.30161
Peak Hip Extension	-11.32	-11.10	-16.0932
Ankle Kinematics (º)			
Peak Ankle Flexion	10.89	11.53	7.52
PeakAnkle Extension	-19.17	-18.97	-17.08
Prosthetic Limb			
Biomechanical Variables	F0E0	F90E90	F180E180
Knee Kinematics (º)			
Peak Knee Flexion (early stance)	10.78	10.93	15.19
Knee Flexion (at opposite heel strike)	8.90	9.54	12.69
Peak Knee Flexion (swing)	52.95	52.98	51.50
Knee Kinematics (N•m/kg)			8.57
Peak Knee Flexion Moment (early stance)	0.03	0.04	0.11
Hip Power (W/kg)			
H1 Power Maximum	1.13	1.10	1.05
H3 Power Maximum	0.73	0.76	0.85
Knee Power (W/kg)			
K1 Power Minimum	-0.07	-0.06	-0.28

K3 Power Minimum	-2.00	-2.06	-2.45
Ankle Power (W/kg)			
A2 Power Maximum	2.86	2.94	3.00
Vertical GRF			
Peak GRF from 10%-30% of gait cycle (% BW)	124.01	123.57	121.14
Time of Peak GRF (s)	0.15	0.15	0.15
Hip Kinematics (º)			
Peak Hip Flexion	28.88	29.11	32.91
Peak Hip Extension	-5.83	-5.59	-0.40
Ankle Kinematics (º)			
Peak Ankle Flexion	18.12	18.35	18.65
PeakAnkle Extension	-5.56	-5.53	-4.97

Note: Walking speed: 1.325 m/s
Gait cycle: 1.14 s

APPENDIX F

Kinetics and kinematics comparison of actual patients and simulation based on varios damping setting of the Mauch S-N-S prosthetic knee at fast walking

Prosthetic Limb			
Biomechanical Variables	f0e0	f90e90	f180e180
Knee Kinematics (º)			
Peak Knee Flexion (early stance)	29.22649	29.25	30.42
Knee Flexion (at opposite heel strike)	5.24	5.14	3.46
Peak Knee Flexion (swing)	66.84	66.79	65.99
Knee Kinematics (N•m/kg)			77.04
Peak Knee Flexion Moment (early stance)	1.04	1.04	1.03
Hip Power (W/kg)			
H1 Power Maximum	4.05	4.16	5.46
H3 Power Maximum	1.24	1.25	1.26
Knee Power (W/kg)			
K1 Power Minimum	-1.71	-1.69	-1.78
K3 Power Minimum	-0.76	-0.76	-0.79
Ankle Power (W/kg)			
A2 Power Maximum	3.08	3.09	3.22
Vertical GRF			
Peak GRF from 10%-30% of gait cycle (% BW)	145.60	146.39	162.38
Time of Peak GRF (s)	0.11	0.11	0.11
Hip Kinematics (º)			
Peak Hip Flexion	39.32	39.42	41.97396
Peak Hip Extension	-16.32	-16.51	-17.2985
Ankle Kinematics (º)			
Peak Ankle Flexion	13.82	13.73	12.57
PeakAnkle Extension	-22.63	-22.79	-24.97
Prosthetic Limb			
Biomechanical Variables	f0e0	f90e90	f180e180
Knee Kinematics (º)			
Peak Knee Flexion (early stance)	14.20	14.30	15.82
Knee Flexion (at opposite heel strike)	12.03	12.41	15.39
Peak Knee Flexion (swing)	53.66	53.27	49.51
Knee Kinematics (N•m/kg)			15.36
Peak Knee Flexion Moment (early stance)	0.12	0.12	0.20
Hip Power (W/kg)			
H1 Power Maximum	1.41	1.40	1.72
H3 Power Maximum	1.13	1.16	1.06
Knee Power (W/kg)			

K1 Power Minimum	-0.21	-0.22	-0.47
K3 Power Minimum	-2.27	-2.31	-2.62
Ankle Power (W/kg)			
A2 Power Maximum	3.24	3.25	3.03
Vertical GRF			
Peak GRF from 10%-30% of gait cycle (% BW)	153.91	153.65	156.4288
Time of Peak GRF (s)	0.11	0.11	0.11
Hip Kinematics (º)			
Peak Hip Flexion	30.65	30.57	33.20
Peak Hip Extension	-5.71	-5.37	-0.94
Ankle Kinematics (º)			
Peak Ankle Flexion	18.33	18.39	17.91
PeakAnkle Extension	-6.36	-6.30	-5.43

Note: Walking speed: 1.682 m/s
Gait cycle: 0.975 s